

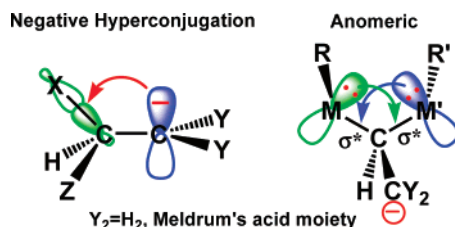
Role of Negative Hyperconjugation and Anomeric Effects in the Stabilization of the Intermediate in S_NV Reactions

Miriam Karni,^{*,†} Claude F. Bernasconi,[‡] and Zvi Rappoport[§]

Schulich Faculty of Chemistry and The Lise Meitner-Minerva Center for Computational Quantum Chemistry, Technion-Israel Institute of Technology, Haifa 32000, Israel, Department of Chemistry and Biochemistry, University of California, Santa Cruz, California 94064, and Department of Organic Chemistry and The Lise Meitner-Minerva Center for Computational Quantum Chemistry, The Hebrew University of Jerusalem, Jerusalem 91904, Israel

chrmiri@tx.technion.ac.il

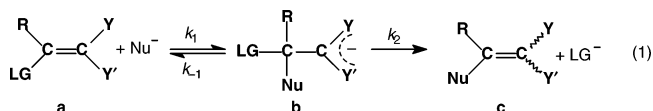
Received August 9, 2007



The role of negative hyperconjugation and anomeric and polar effects in stabilizing the $XZHC^\beta C^\alpha YY'^-$ intermediates in S_NV reactions was studied computationally by DFT methods. Destabilizing steric effects are also discussed. The following ions were studied: $X = CH_3O, CH_3S, CF_3CH_2O$ and $Y = Y' = Z = H$ (**7b–7d**), $Y = Y' = H, Z = CH_3O, CH_3S, CF_3CH_2O$ (**7e–7i**), $YY' =$ Meldrum's acid-like moiety (Mu), $Z = H$, (**8b–8d**), and $YY' = Mu, Z = CH_3O, CH_3S, CF_3CH_2O$ (**8e–8i**). The electron-withdrawing Mu substituent at C^α stabilizes considerably the intermediates and allows their accumulation. The hyperconjugation ability (HCA) (i.e., the stabilization due to $2p(C^\alpha) \rightarrow \sigma^*(C^\beta-X)$ interaction) in **8b–8d** follows the order (for X, kcal/mol) CH_3S (8.5) > CF_3CH_2O (7.6) \approx CH_3O (7.5). The HCA in **8b–8d** is significantly smaller than that in **7b–7d** due to charge delocalization in Mu in the former. The calculated solvent (1:1 DMSO/H₂O) effect is small. The stability of disubstituted ions (**7e–7i** and **8e–8i**) is larger than that of monosubstituted ions due to additional stabilization by negative hyperconjugation and an anomeric effect. However, steric repulsion between the geminal C^β substituents destabilizes these ions. The steric effects are larger when one or both substituents are CH_3S . The anomeric stabilization (the energy difference between the *anti,anti* and *gauche,gauche* conformers) in the disubstituted anions contributes only a small fraction to their total stabilization. Its order (for the following X/Z pairs, kcal/mol) is CF_3CH_2O/CH_3S (**8i**, 4.9) > CF_3CH_2O/CH_3O (**8h**, 3.9) > CH_3O/CH_3S (**8g**, 3.3) > CH_3S/CH_3S (**8f**, 2.9) > CH_3O/CH_3O (**8e**, 2.4). Significantly larger anomeric effects of ca. 8–9 kcal/mol are calculated for the corresponding conjugate acids.

Introduction

A. Experimental Background. The past few years increased considerably our understanding of structure–reactivity relationships in S_NV reactions that proceed by the two-step mechanism shown in eq 1.



This mechanism is favored for reactions of nucleophiles (Nu^-) with substrates activated by electron-withdrawing groups (EWGs) Y and Y' .¹ The progress has mainly come from studying systems where the nucleophilic addition step is thermodynamically

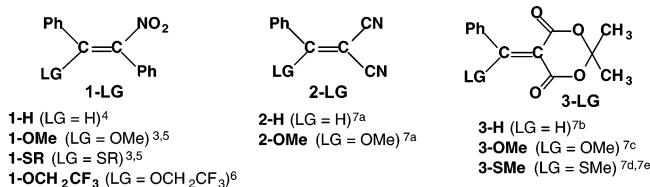
[†] Technion-Israel Institute of Technology.

[‡] University of California.

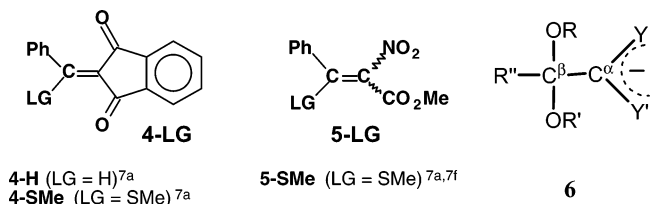
[§] The Hebrew University of Jerusalem.

favorable ($K_1[\text{Nu}^-] \gtrsim 1$) and the leaving group (LG^-) loss is slower than the nucleophilic attack ($k_1[\text{Nu}^-] \gtrsim k_2$). When these conditions are met, the intermediate accumulates to detectable levels which allow a kinetic determination of all rate constants (k_1 , k_{-1} , and k_2) in eq 1.

The first system that yielded such a detectable intermediate and involved a vinylic substrate with a “real” leaving group² was the reaction of β -methoxy- α -nitrostilbene, **1-OMe**, with



thiolate ions.³ Subsequently, several other systems have permitted the direct measurement of these individual rate constants as a function of the nucleophile, R, LG, Y, and Y'. This has led to a better understanding of the major factors that govern the reactivity in these reactions. Substrates that have been investigated so far are **1-LG**,^{4–6} **2-LG**,^{7a} **3-LG**,^{7b–e} **4-LG**,^{7a} and **5-LG**.^{7a,f} Most studies have been performed in 1:1 DMSO/H₂O



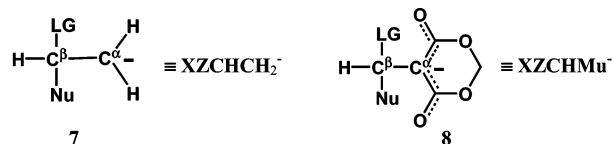
(v/v) with thiolate ions, alkoxide ions, and amines as nucleophiles. These studies have shown a rather complex interplay of factors that influence the reactivity, including inductive/resonance effects of the activating groups, π donor effects of the nucleofuge, steric effects, polarizability effects, and, presumably, hyperconjugative (anomeric) effects of the nucleofuges and the nucleophiles.

The complexity of this interplay is increased by the influence of these factors on the thermodynamics of intermediate forma-

tion, i.e., the equilibrium constant $K_1 = k_1/k_{-1}$, which often differs from their influence on the rate constants. This is because resonance effects of Y and Y' enhance K_1 but reduce k_1 and k_{-1} due to increased intrinsic barriers^{8a,b} associated with the resonance effects.⁹

Perhaps the least understood aspect of these reactions is the role played by the negative hyperconjugation¹⁰ and anomeric effect (see below).¹¹ The anomeric effect was assumed to play a significant role in the reactions of **1-OMe** or **1-OCH₂CF₃** with OH[−] and CF₃CH₂O[−].^{5a,6} With these nucleophiles, k_1 for the reaction with **1-OMe** or **1-OCH₂CF₃** is about the same as for the reactions with **1-H**, suggesting that the stabilization of the reactant by π -donation from the CH₃O or CF₃CH₂O group is offset by the hyperconjugative (including anomeric) stabilization of the transition state leading to the reaction intermediate (e.g., **6**). A similar situation exists for the reactions of alkoxide ions and OH[−] with **3-OMe**^{7c} although, due to the concurrent operation of steric, inductive, and π donor effects, it is difficult to sort out the relative contribution of the hyperconjugative effects. This contrasts with the much slower reactions of HOCH₂CH₂S[−] or piperidine⁶ with **1-OMe** or **1-OCH₂CF₃** than their reactions with **1-H**, apparently because there is no compensation for the π donor stabilization of the precursor by the additional hyperconjugative (including anomeric) effects in the charged transition state.

B. Negative Hyperconjugation and Anomeric Stabilization in XZCHCY_2^- . The intermediate carbanions in the S_NV reaction, i.e., **7** and **8** (or in general **9a**), can be stabilized



LG, Nu = a) H, H; b) H, CH₃O; c) H, CH₃S; d) H, CF₃CH₂O; e) CH₃O, CH₃O; f) CH₃S, CH₃S; g) CH₃O, CH₃S; h) CH₃O, CF₃CH₂O; i) CH₃S, CF₃CH₂O

electronically by a proper combination of X, Z, and Y substituents. The stability and conformation of the anions are determined mainly by a combination of the following effects: (a) negative hyperconjugation between the lone pair electrons in the 2p(C α) orbital and the C β –X, C β –Z, and C β –H σ^* orbitals;¹⁰ (b) anomeric effect between X and Z bearing a lone pair of electrons, e.g., in dialkoxy intermediates such as **6**;^{11,12} (c) stabilization by inductive/ π donor effects of electron-

(8) (a) The intrinsic barrier of a reaction refers to the barrier in the absence of a thermodynamic driving force.^{8b} (b) Marcus, R. A. *J. Phys. Chem.* **1968**, 72, 891.

(9) (a) Bernasconi, C. F. *Acc. Chem. Res.* **1987**, 20, 301. (b) Bernasconi, C. F. *Acc. Chem. Res.* **1992**, 25, 9. (c) Bernasconi, C. F. *Adv. Phys. Org. Chem.* **1992**, 27, 119.

(10) (a) Hoffmann, R.; Radom, L.; Pople, J. A.; Schleyer, P. v. R.; Hehre, W. J.; Salem, L., *J. Am. Chem. Soc.* **1972**, 94, 6221. (b) Radom, L.; Hehre, W. J.; Pople, J. A. *J. Am. Chem. Soc.* **1972**, 94, 2371.

(11) (a) Kirby, A. G. *The Anomeric Effect and Related Stereoelectronic Effects of Oxygen*; Springer-Verlag: Berlin, 1983. (b) Jeffrey, G. A.; Pople, J. A.; Radom, L. *Carbohydr. Res.* **1972**, 25, 117. (c) Jeffrey, G. A.; Pople, J. A.; Radom, L. *Carbohydr. Res.* **1974**, 38, 81. (d) Jeffrey, G. A.; Pople, J. A.; Binkley, J. S.; Vishveshwara, S. *J. Am. Chem. Soc.* **1978**, 100, 373. (e) Schleyer, P. v. R.; Jemmis, E. D.; Spitznagel, G. W. *J. Am. Chem. Soc.* **1985**, 107, 6393. (f) Wiberg, K. B.; Murcko, M. A. *J. Am. Chem. Soc.* **1989**, 111, 4821. (g) Zalzner, U.; Schleyer, P. v. R. *J. Am. Chem. Soc.* **1993**, 115, 10231. (h) Kneisler, J. R.; Allinger, N. L. *J. Comput. Chem.* **1996**, 17, 757. (i) Chang, Y.-P.; Su, T.-M. *J. Phys. Chem. A* **1999**, 103, 8706. (j) Yokoyama, Y.; Ohashi, Y. *Bull. Chem. Soc. Jpn.* **1999**, 72, 2183. See also references cited in the papers above.

(1) Reviews on the S_NV mechanism: (a) Rappoport, Z. *Adv. Phys. Org. Chem.* **1969**, 7, 1. (b) Modena, G. *Acc. Chem. Res.* **1971**, 4, 73. (c) Miller, S. I. *Tetrahedron* **1977**, 33, 1211. (d) Rappoport, Z. *Acc. Chem. Res.* **1981**, 14, 7; **1992**, 25, 474. (e) Rappoport, Z. *Recl. Trav. Chim. Pays-Bas* **1985**, 104, 309. (f) Shainyan, B. *Usp. Khim.* **1986**, 55, 942. (g) Okuyama, T.; Lodder, G. *Adv. Phys. Org. Chem.* **2002**, 37, 1.

(2) In contrast to the LG being an alkyl group, phenyl group, or hydrogen.

(3) (a) Bernasconi, C. F.; Fassberg, J.; Killion, R. B., Jr.; Rappoport, Z. *J. Am. Chem. Soc.* **1989**, 111, 6962. (b) Bernasconi, C. F.; Fassberg, J.; Killion, R. B., Jr.; Rappoport, Z. *J. Am. Chem. Soc.* **1990**, 112, 3169.

(4) Bernasconi, C. F.; Killion, R. B., Jr. *J. Am. Chem. Soc.* **1988**, 110, 7506.

(5) (a) Bernasconi, C. F.; Fassberg, J.; Killion, R. B., Jr.; Schuck, D. F.; Rappoport, Z. *J. Am. Chem. Soc.* **1991**, 113, 4937. (b) Bernasconi, C. F.; Leyes, A. E.; Eventova, I.; Rappoport, Z. *J. Am. Chem. Soc.* **1995**, 117, 1703.

(6) Bernasconi, C. F.; Schuck, D. F.; Ketner, R. J.; Weiss, M.; Rappoport, Z. *J. Am. Chem. Soc.* **1994**, 116, 11764.

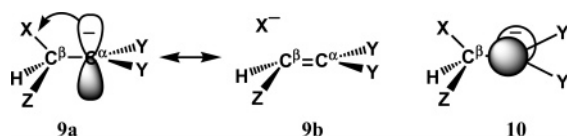
(7) (a) Bernasconi, C. F.; Ketner, R. J.; Ragains, M. L.; Chen, X.; Rappoport, Z. *J. Am. Chem. Soc.* **2001**, 123, 2155. (b) Bernasconi, C. F.; Ketner, R. J. *J. Org. Chem.* **1998**, 63, 6266. (c) Bernasconi, C. F.; Ketner, R. J.; Chen, X.; Rappoport, Z. *J. Am. Chem. Soc.* **1998**, 120, 7461. (d) Bernasconi, C. F.; Ketner, R. J.; Chen, X.; Rappoport, Z. *Can. J. Chem.* **1999**, 77, 584. (e) Bernasconi, C. F.; Ketner, R. J.; Chen, X.; Rappoport, Z. *ARKIVOK* **2002**, xii, 161. (f) Bernasconi, C. F.; Brown, S. D.; Eventova, I.; Rappoport, Z. *J. Org. Chem.* **2007**, 72, 3302.

withdrawing substituents on C^α (e.g., $Y_2 = (CN)_2$ or Meldrum's acid moiety (see below); (d) destabilization caused by steric repulsion between the geminal C^β substituents.

In $XCH_2CY_2^-$ (e.g., **7b-d**, **8b-d**) the relative energy $\Delta E(\theta)$ of any rotational conformation can be calculated by eq 2, where

$$\Delta E(\theta) = 0.5V_X(1 - \cos 2\theta) \quad (2)$$

V_X is the hyperconjugative ability (HCA) of the substituent X and θ is the $XCCY$ dihedral angle.^{10b,13} The maximal hyperconjugative stabilization is achieved when $\theta = 90^\circ$, a conformation in which the $2p(C^\alpha)$ orbital eclipses the $\sigma^*(C^\beta-X)$ orbital (**9a**, $Z = H$), leading to the most stable conformer. The least stable conformation is when $\theta = 0^\circ$ and the $2p(C^\alpha)$ orbital is orthogonal to the $\sigma^*(C^\beta-X)$ orbital (**10**, $Z = H$). The HCA of a substituent is the energy difference between **10** and **9a**. The negative hyperconjugation in **9a** leads to the elongation of the $X-C^\beta$ bond and shortening of the $C^\beta-C^\alpha$ bond due to the contribution of resonance form **9b**.^{10a}

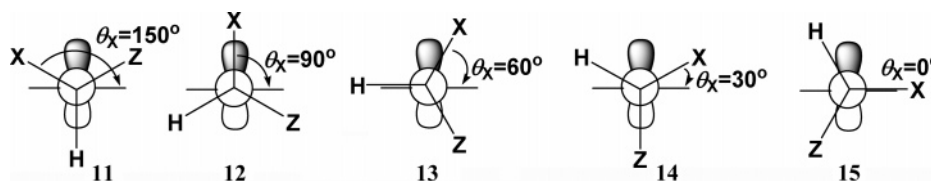


Equation 2 can be extended to β -polysubstituted anions.^{13a} The relative energy of a particular rotational conformer of $XXZCHCY_2^-$ can be calculated from eq 3, where θ is the $XCCY$

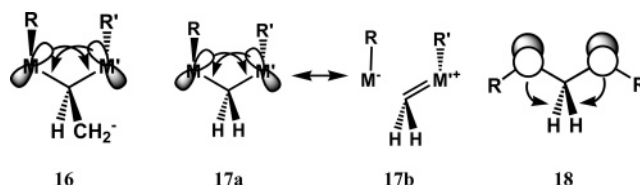
$$\Delta E(\theta) = 0.5V_X(1 - \cos 2\theta) + 0.5V_H(1 - \cos 2(\theta + 120^\circ)) + 0.5V_Z(1 - \cos 2(\theta + 240^\circ)) \quad (3)$$

dihedral angle and V_X , V_H , and V_Z are the HCAs of the β substituents X, H, and Z in $XCH_2CY_2^-$, $CH_3CY_2^-$, and $ZCH_2CY_2^-$, respectively; e.g., V_X is the rotational barrier of **9a** ($Z = H$) \rightarrow **10** ($Z = H$). Equation 3 assumes full additivity of substituent effects but neglects dipolar interactions, direct interactions between X and Z, and steric effects.^{13b}

When two β substituents with relatively high HCAs are involved, the hyperconjugative interaction never vanishes, since a rotation decreasing the hyperconjugative contribution of one substituent moves the second one to an orientation that increases its hyperconjugative interaction. Thus, for $XXZCHCH_2^-$ (ignoring the very small HCA of hydrogen ($V_H = 0.03$ kcal/mol)),¹⁴ the hyperconjugative contribution of both substituents is $0.25V_X + 0.25V_Z$ ($\theta_X = 150^\circ$, **11**), $V_X + 0.25V_Z$ ($\theta_X = 90^\circ$, **12**), $0.75V_X + 0.75V_Z$ ($\theta_X = 60^\circ$, **13**), $0.25V_X + V_Z$ ($\theta_X = 30^\circ$, **14**), and $0.75V_Z$ ($\theta_X = 0^\circ$, **15**). For $V_X = V_Z$, the most and least stable conformers are at $\theta_X = 60^\circ$ and $\theta_X = 150^\circ$, respectively.



When both X and Z have a lone pair there is a mutual hyperconjugative stabilizing interaction between them. This is the anomeric interaction¹¹ which is not taken into account by eq 3. The lone pair on X interacts with the $\sigma^*(C^\beta-Z)$ orbital, and the lone pair on Z interacts with the $\sigma^*(C^\beta-X)$ orbital (**16**, X, Z = RM, R'M'). Its extent depends on the mutual alignment of the R'M' and RM bonds (i.e., the RMCM' and R'M'CM dihedral angles, e.g., **17a** and **18**). In $H_2C(MH)M'H^-$ ($M = M' = O, S$), the largest stabilizing anomeric interaction was calculated for the C_2 symmetry *gauche,gauche* (*g,g*) conformation where $\theta(HMCM') = \theta(H'M'CM) = 60^\circ$ (**17a**, $R = R' = H$), which enables the $p(M) \rightarrow \sigma^*(C-M')$ delocalization (the arrows in **16**, **17a**, and **18** indicate the direction of electron delocalization). The least stable conformer is the *anti,anti* (*a,a*) conformer where $\theta(H'M'CM) = \theta(HMCM') = 180.0^\circ$ (**18**, $R = R' = H'$), where such delocalization is prevented due to the absence of a proper orbital overlap.^{11g}



A geometric consequence of the anomeric interaction is a shortening of the $C-M'$ bond and lengthening of the $C-M$ bond. This was ascribed to the acquisition of some double bond character in the $C-M'$ bond and the delocalization of electrons into the antibonding $\sigma^*(C-M)$ orbital (cf. structure **17b**).¹¹ In the *a,a* conformation of dimethoxymethane (**18**, $R = R' = CH_3$), the $C-O$ bond length is 1.395 Å. In the *g,g* conformation each of the equivalent $C-O$ bonds acts simultaneously as a π donor and a σ^* acceptor. One effect will shorten the bond, while the second will lengthen it, leading to a $C-O$ bond length of 1.404 Å. In the *a,g* conformation ($\angle R'M'CM = 180.0^\circ$ and $\angle RMCM' = 60.0^\circ$), where only M can act as a donor and R'M' is the acceptor, the donor $C-O$ bond length is 1.385 Å, shorter than in both former conformations, while the acceptor $C-O$ bond is longer, 1.414 Å (calculated at B3LYP/6-31G(d,p)).^{11h} Another feature which depends on the RMCM' angle is the marked decrease in the MCM' angle upon rotation from the *g,g* conformation to the *a,g* conformation and to the *a,a* conformation. For example, for $CH_3OCH_2OCH_3$, the calculated OCO bond angles are 114.4° (*g,g*; X-ray: 113.7° ^{11j}), 110.0° (*a,g*), and 106.0° (*a,a*) (at B3LYP/6-31G(d,p)).^{11h} The larger MCM' angle in the *g,g* conformation was attributed to a relief of the steric congestion, but stereoelectronic effects, e.g., change in hybridization, are also to be considered.^{11a}

$XXZCHCY_2^-$ anions are actually trisubstituted methanes, $XXZCHR$,¹⁵ where the substituents X, Z (e.g., OR', SR', etc.), and R (e.g., CH_2^-) have lone pair electrons which interact with the σ^* orbitals of the $C-X$, $C-R$, or $C-Z$ bonds having a proper orientation. Thus, the interactions designated above as negative hyperconjugation of the anionic lone pair with the C^β substituent bonds can be viewed as anomeric interactions (or

vice versa). However, the anionic lone pair is a significantly stronger donor than the lone pairs on O or S; thus, it will act as the π donor, and the C–X/Z bonds will be the σ^* acceptors. Consequently, we also expect that the stabilization due to the interaction of $2p(C^\alpha)$ electrons with $\sigma^*(C-X/Z)$ will be more dominant than that caused by the mutual anomeric interactions between the C^β substituents. Thus, the most stable conformations and the stabilization energies will be governed by a delicate interplay of the interactions between the three lone pair (“anomeric”) centers. In this study we try to estimate the importance of each of the conjugative/anomeric effects to the stability of the S_NV reaction intermediates and the additional stabilization bestowed upon the anion by a second C^β substituent bearing a lone pair electron (i.e., LG = CH_3O , CH_3S , or CF_3-CH_2O vs LG = H). To do this, we present a density functional study of the structures and thermodynamic stabilities of models of the intermediates in the experimental S_NV reactions (**b**, eq 1). We discuss first the structures and stabilities of carbanions **7a–7i** that will serve as reference systems and then those of **8a–8i**, the models for the experimental carbanions in which the anionic center is stabilized by Meldrum’s acid. We will mainly discuss the calculated stabilizing effects in the gas phase which reflect the inherent stabilizing effects. For **7b–7d** and **8b–8i**, which model experimental systems, we will also provide solvent effects calculated using the polarized continuum model (PCM; see below). The Meldrum’s acid-like substituent in **8** will be indicated by the abbreviation “Mu”.

Computational Methods

The calculations were performed using the G98 and G03 series of programs.¹⁶ The structures were fully optimized using the hybrid B3LYP density functional¹⁷ with the 6-31++G(d,p) basis set.¹⁸ Analytic frequencies were calculated to identify the structures as minima on the PES. The reported relative energies include the contribution of zero-point vibrational energies (ZPE). Charges were calculated using natural population analysis (NPA) embedded in the NBO program.^{19a} The stabilization energy associated with the hyperconjugation and electron delocalization from i to j NBOs is

estimated by $\Delta E_{ij} = q_i F(i,j)^2 / (\epsilon_j - \epsilon_i)$, where q_i is the occupancy in the donor orbital, $F(i,j)$ is the off-diagonal NBO Fock matrix element (which reflects the overlap between the donor and acceptor orbitals) and ϵ_i and ϵ_j are the natural bond orbital energies.^{19b} The calculated thermodynamic stabilities refer to the gas phase unless stated otherwise. For **7b–7d** and **8b–8i** we have also calculated the effect of a 1:1 DMSO/H₂O solvent using the PCM solvation model²⁰ with the united atom topological model (UAHF; applied on atomic radii optimized at HF/6-31G*)^{21a–e} with a dielectric constant of 74.2.^{21f} For calculating the solvent effect, we have used the gas-phase-optimized geometries. Geometry optimization of selected anions using the PCM model or explicitly adding water molecules did not reveal any significant changes in geometries and solvation energies.²²

Results and Discussion

A. $XZCHCH_2^-$ (7a–7i). a. Geometry. Schematic drawings of the structures of the most stable conformers of **7a–7i** and their important geometric features are given in Table 1. For comparison, important geometric parameters of **7en–7in**, the neutral conjugate acids of **7e–7i**, are given in Table 2. The atom numbering is as specifically indicated in the table footnotes.

Due to the strong negative hyperconjugation between the $2p(C^\alpha)$ lone pair orbital and the $\sigma^*(C^\beta-X)$ and $\sigma^*(C^\beta-Z)$ orbitals, **7b–7d** and **7f–7i** are unstable and dissociate spontaneously upon geometry optimization to $HZC=CH_2 + X^-$.²³ To evaluate the relative stabilizing effects in **7**, we prevented these dissociations by artificially freezing $r(C-O)$ in **7b**, **7d**, **7g**, **7h**, and **7i** to 1.425 Å and $r(C-S)$ in **7c**, **7f**, **7g**, and **7i** to 1.86 Å. These are the average bond length values in their corresponding conjugate acids.

In the discussion of the geometries we emphasize the geometrical features which are relevant to the various hyperconjugative/anomeric interactions in these anions. However, due to the constrained values of $r(C^\beta-X/Z)$ it is not possible to analyze the changes in these bond lengths imposed by hyperconjugation and anomeric interactions. All anions **7a–7i** have a pyramidal anionic center. The $C^\beta-C^\alpha$ bond lengths in **7b–7i** are 1.45–1.48 Å, significantly shorter than that in **7a** ($X = H$)

(12) (a) Hine, J.; Klueppel, A. W. *J. Am. Chem. Soc.* **1974**, *96*, 2924. (b) Wiberg, K. B.; Squires, R. R. *J. Chem. Thermodyn.* **1979**, *11*, 773. (c) Harcourt, M. P.; More O’Ferrall, R. A. *Bull. Soc. Chim. Fr.* **1988**, 407.

(13) (a) Apeloig, Y.; Rappoport, Z. *J. Am. Chem. Soc.* **1979**, *101*, 5095. (b) Equation 2 includes only the 2-fold component of a more general equation suggested in ref 10b.

(14) Calculated from the rotation barrier of **9** \rightarrow **10** ($X = Z = Y = H$, $H_3CCH_2^-$).

(15) (a) Lathan, W. A.; Radom, L.; Hehre, W. J.; Pople, J. A., *J. Am. Chem. Soc.* **1973**, *95*, 699. (b) Scott, C.; Grein, F. *Can. J. Chem.* **1994**, *72*, 2521.

(16) Gaussian 98 (revision A.11) and Gaussian 03 (revision B.05): M. J. Frisch, et al., Gaussian, Inc., Pittsburgh, PA, 2001. The complete reference is given in the Supporting Information.

(17) (a) Koch, W.; Holthausen, M. C. *A Chemist’s Guide to Density Functional Theory*; Wiley-VCH: New York, 2000. (b) Parr, R. G.; Yang, W. *Density-Functional Theory of Atoms and Molecules*; Oxford University Press: New York, 1989. (c) Stephens, P. J.; Devlin, F.; Chabalowski, C. F.; Frisch, M. J. *J. Phys. Chem.* **1994**, *98*, 11623. (d) Hertwig, R. H.; Koch, W. *Chem. Phys. Lett.* **1997**, *268*, 345. (e) Becke, A. D. *J. Chem. Phys.* **1993**, *98*, 5648. (f) Becke, A. D. *Phys. Rev. A* **1988**, *38*, 3098. (g) Lee, C.; Yang, W.; Parr, R. G. *Phys. Rev. B* **1988**, *37*, 785.

(18) The basis set and corresponding references are provided at <http://www.emsl.pnl.gov/forms/basisform.html>.

(19) (a) NBO, v 5.0: Glendening, E. D.; Badenhoop, J. K.; Reed, A. E.; Carpenter, J. E.; Bohmann, J. A.; Morales, C. M.; Weinhold, F., Theoretical Chemistry Institute, University of Wisconsin, Madison, WI, 2001; <http://www.chem.wisc.edu/~nbo5>. (b) Weinhold, F.; Clark, L., *Valence and Bonding. A Natural Bond Orbital Donor-Acceptor Perspective*; Cambridge University Press: Cambridge, U.K., 2005.

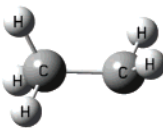
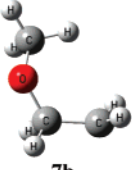
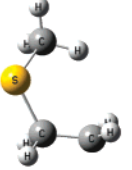
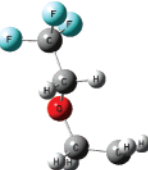
(20) (a) Miertus, S.; Scrocco, E.; Tomasi, J. *Chem. Phys.* **1981**, *55*, 117. (b) Cancès, M. T.; Mennucci, B.; Tomasi, J. *J. Chem. Phys.* **1997**, *107*, 3032. (c) Cossi, M.; Scalmani, G.; Rega, N.; Barone, V. *J. Chem. Phys.* **2002**, *117*, 43.

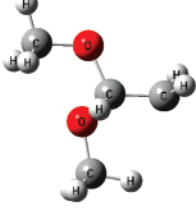
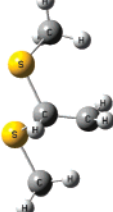
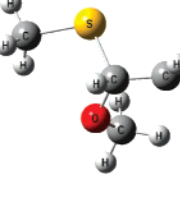
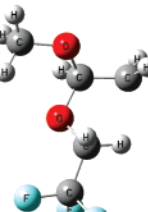
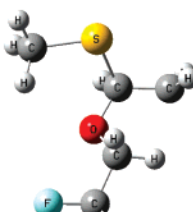
(21) (a) To test the reliability of this method for calculating pK_a values and stabilization trends in our systems, we calculated pK_a differences (ΔpK_a) in water solution between HA and HB according to $HA + B^- \rightarrow HB + A^-$. $\Delta pK_a = (\Delta G_{\text{gas}} - \Delta G_{\text{solv}})/2.3RT$ ($T = 298$ K).^{21b} $\Delta pK_a(CF_3CH_2OH-CH_3OH) = -5.3$ (experimental -3.1).^{21c,d} $\Delta pK_a(\text{Meldrum acid (19b)} - CF_3CH_2OH) = -6.2$ (experimental -7.6).^{21c,d} and $\Delta pK_a(\text{Meldrum acid (19b)} - CH_3OH) = -11.6$ (experimental -10.7).^{21c,d} Part of the computational error results from errors in the computed ΔG_{gas} . However, the trends are well reproduced.^{21e} (b) Almerindo, G. I.; Tondo, D. W.; Pliego, R., Jr. *J. Phys. Chem. A* **2004**, *108*, 166. (c) Bartmess, J. E.; Scott, J. A.; McIver, R. T., Jr. *J. Am. Chem. Soc.* **1979**, *101*, 6056. (d) Bordwell, F. G. *Acc. Chem. Res.* **1988**, *21*, 456. (e) Schüürmann, G.; Cossi, M.; Barone, V.; Tomasi, J. *J. Phys. Chem. A* **1998**, *102*, 6706. (f) Kaatz, U.; Pottel, R.; Schafer, M. *J. Phys. Chem.* **1989**, *93*, 5623.

(22) For example, the difference in the total free energy in solution of **8b** calculated using the optimized structure in solution and in the gas phase is 0.6 kcal/mol. The following structural parameters of **8b** were calculated in the gas phase and solution, respectively: $r(C^\beta-C^\alpha) = 1.499$ and 1.497 Å, $r(C^\beta-O) = 1.453$ and 1.456 Å, $\angle OCB^\alpha = 114.9^\circ$ and 116.0° , $\angle COCB^\alpha = -69.3^\circ$ and -65.9° .

(23) **7a** and **7e** did not dissociate, but the lengths of the H^0-C (in **7a**) and O^1-C (**7e**) bonds are 1.137 and 1.520 Å, respectively, significantly longer than those of the H^2-C^β and O^2-C^β bonds of 1.105 and 1.426 Å, respectively.

TABLE 1. Schematic Structures and Selected Geometry Parameters^a of XZCHCH₂⁻ (X, Z = H, CH₃O, CH₃S, and CF₃CH₂O)^{b,c}

Geometry parameters	 7a	 7b	 7c	 7d
$r(C^{\beta}-C^{\alpha})$	1.527	1.482	1.473	1.471
$r(O/S-C^{\beta})$	1.137 ^d	1.425 ^e	1.860 ^e	1.425 ^e
$r(C^1-O/S)$	—	1.403	1.823	1.389
$\angle(O/S)C^{\beta}C^{\alpha}$	118.73 ^d	121.44	122.2	121.18
$\angle C^1(O/S)C^{\beta}C^{\alpha}$	—	61.1	51.2	54.74
$\angle(O/S)C^{\beta}C^{\alpha}H^1$	60.3 ^d (0.0) ^f	62.6 (5.6) ^f	60.8 (7.2) ^f	64.9 (7.3) ^f
$\angle H^1C^{\alpha}C^{\beta}H^2$	120.6	136.3	135.9	144.3

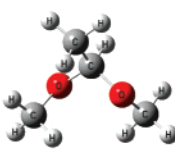
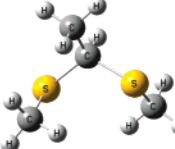
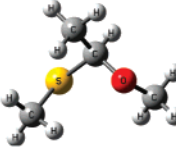
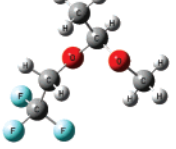
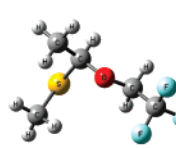
Geometry parameters	 7e	 7f	 7g	 7h	 7i
$r(C^{\beta}-C^{\alpha})$	1.471	1.454	1.457	1.476	1.465
$r(O^1/S^1-C^{\beta})$	1.425 ^e	1.860 ^e	1.860 ^e	1.425 ^e	1.860 ^e
$r(O^2/S^2-C^{\beta})$	1.425 ^e	1.860 ^e	1.425 ^e	1.425 ^e	1.425 ^e
$r(C^1-O^1/S^1)$	1.415	1.821	1.826	1.415	1.854
$r(C^2-O^2/S^2)$	1.408	1.831	1.413	1.398	1.398
$\angle(O^1/S^1)C^{\beta}(O^2/S^2)$	(107.0) ^g 102.7 (97.4) ^h	(109.9) ^g 101.5 (99.1) ^h	(108.1) ^g 99.4 (96.3) ^h	(105.7) ^g 105.7 (97.0) ^h	(106.5) ^g 106.7 (96.4) ^h
$\angle(O^1/S^1)C^{\beta}C^{\alpha}$	115.33	122.23	119.52	113.0	110.99
$\angle(O^2/S^2)C^{\beta}C^{\alpha}$	114.91	115.14	118.25	116.40	118.11
$\angle C^1(O^1/S^1)C^{\beta}C^{\alpha}$	174.7	40.7	-41.26	175.8	-171.4
$\angle C^2(O^2/S^2)C^{\beta}C^{\alpha}$	63.3	42.7	-39.55	32.4	36.2
$\angle C^1(O^1/S^1)C^{\beta}(O^2/S^2)$	59.5	-89.2	-171.5	-55.7	-41.4
$\angle C^2(O^2/S^2)C^{\beta}(O^1/S^1)$	170.6	176.9	91.5	-93.9	-89.6
$\angle(O^1/S^1)C^{\beta}C^{\alpha}H^1$	-47.6 (16.2) ^f	-60.0 (11.4) ^f	-43.5 (27.9) ^f	26.5 (36.6) ^f	33.7 (33.9) ^f
$\angle(O^2/S^2)C^{\beta}C^{\alpha}H^1$	71.6 (135.4) ^f	63.8 (135.2) ^f	77.7 (149.1) ^f	-96.2 (159.3) ^f	-90.0 (157.6) ^f
$\angle H^1C^{\alpha}C^{\beta}H^2$	127.5	142.7	142.7	126.2	135.2

^a Bond lengths in angstroms, bond angles in degrees, at B3LYP/6-31++G(d,p). ^b For the most stable conformer. ^c For atom numbering use the following formulas: **7a**, H⁰C^βH₂C^αH¹H²-; **7b**, C¹H₃OC^βH₂C^αH¹H²-; **7c**, C¹H₃SC^βH₂C^αH¹H²-; **7d**, CF₃C¹H₂OC^βH₂C^αH¹H²-; **7e**, C¹H₃O¹(C²H₃O²)C^βH₂C^αH¹H²-; **7f**, C¹H₃O¹(C²H₃S²)C^βH₂C^αH¹H²-; **7g**, C¹H₃S¹(C²H₃O²)C^βH₂C^αH¹H²-; **7h**, C¹H₃O¹(CF₃C²H₂O²)C^βH₂C^αH¹H²-; **7i**, C¹H₃S¹(CF₃C²H₂O²)C^βH₂C^αH¹H²-. O¹/S¹ and O²/S² are located above and below the C^βC^αH₂ plane, respectively. ^d r(H⁰-C^β), ∠H⁰C^βC^α, and ∠H⁰C^βC^αH¹, respectively. ^e Not optimized. ^f ∠(O¹/S¹)C^βC^αχ and ∠(O²/S²)C^βC^αχ, where χ is a dummy atom on the bisector of the H¹C^αH² angle. This angle exhibits the deviation from eclipsing 2p(C^α) and σ*(C^β-O/S) orbitals. ^g ∠C¹(O¹/S¹)C^β(O²/S²) and ∠C²(O²/S²)C^β(O¹/S¹) = 60°, and ∠H¹C^αC^βH² = 180°. ^h ∠C¹(O¹/S¹)C^β(O²/S²) and ∠C²(O²/S²)C^β(O¹/S¹) = 180.0°, and ∠H¹C^αC^βH² = 180°.

of 1.527 Å where the negative hyperconjugation is negligible and in the neutral conjugate acids (Table 2). These short bond lengths reflect a partial double bond character in C^β-C^α due to the contribution of resonance structure **9b**. The C^β-C^α bond lengths in the monosubstituted anions **7b**–**7d** are longer than

the corresponding bonds in the disubstituted anions **7e**–**7i**, reflecting a larger hyperconjugative interaction in the latter (see below). In anions **7b**–**7d** the X-C^β bond almost eclipses the bisector of the H¹C^αH² angle, enabling good overlap between the 2p(C^α) and σ*(C^β-X) orbitals. The structural rule outlined

TABLE 2. Schematic Structures and Selected Optimized Geometry Parameters^a of $XZCHCH_3$ ($X, Z = CH_3O, CH_3S, \text{ and } CF_3CH_2O$)^{b-d}

Geometry parameters	 7en $C^{\alpha}H_3C^{\beta}H(O^1C^1H_3)(O^2C^4H_3)$	 7fn $C^{\alpha}H_3C^{\beta}H(S^1C^1H_3)(S^2C^4H_3)$	 7gn $C^{\alpha}H_3C^{\beta}H(O^1C^1H_3)(S^2C^4H_3)$	 7hn $C^{\alpha}H_3C^{\beta}H(O^1C^1H_2CF_3)(O^2C^4H_3)$	 7in $C^{\alpha}H_3C^{\beta}H(O^1C^1H_2CF_3)(S^2C^4H_3)$
$r(C^{\alpha}-C^{\beta})$	1.522 (1.531)	1.530 (1.527)	1.523 (1.527)	1.520 (1.530)	1.521 (1.526)
$r(C^{\beta}-O^1/S^1)$	1.413 (1.410)	1.847 (1.850)	1.410 (1.418)	1.433 (1.420)	1.421 (1.427)
$r(C^{\beta}-O^2/S^2)$	1.419 (1.410)	1.846 (1.850)	1.863 (1.852)	1.403 (1.404)	1.885 (1.847)
$r(C^3-O^1/S^1)$	1.424 (1.417)	1.827 (1.828)	1.423 (1.420)	1.412 (1.404)	1.409 (1.407)
$r(C^4-O^2/S^2)$	1.426 (1.417)	1.825 (1.828)	1.830 (1.828)	1.430 (1.420)	1.831 (1.827)
$\angle(O^1/S^1)C^{\beta}(O^2/S^2)$	112.20 (102.4)	115.18 (103.46)	113.3 (101.84)	112.20 (102.12)	113.17 (101.78)
$\angle(C^3(O^1/S^1)C^{\beta}(O^2/S^2))$	64.8 (180.0) ^e	64.5 (180.0) ^e	70.6 (180.0) ^e	61.9 (180.0) ^e	67.4 (180.0) ^e
$\angle(C^4(O^2/S^2)C^{\beta}(O^1/S^1))$	64.8 (180.0) ^e	62.7 (180.0) ^e	62.5 (180.0) ^e	67.8 (180.0) ^e	63.5 (180.0) ^e

^a Bond lengths in angstroms, bond angles in degrees, at B3LYP/6-31++G(d,p). ^b For the most stable conformer. ^c Numbering according to the notations in the column caption. ^d The values in parentheses are for the less stable *a,a* rotamer. ^e Kept constant at 180.0° while all other parameters were optimized.

above that predicts rotamer **13** ($\theta_X = 60^\circ$) to be of the highest stability according to eq 3 is only partially met for the disubstituted anions **7e–7i** as exhibited by the $(O^1/S^1)C^{\beta}C^{\alpha}\chi$ and $(O^2/S^2)C^{\beta}C^{\alpha}\chi$ angles (χ is a dummy atom on the bisector of the $H^1C^{\alpha}H^2$ angle), with a better agreement for **7g–7i** for which the $(O^1/S^1)C^{\beta}C^{\alpha}\chi$ and $(O^2/S^2)C^{\beta}C^{\alpha}\chi$ angles are around 30° and 150° (Table 1).

As shown in Table 1, the anomeric effect between X and Z in **7e–7i** does not dictate a *g,g* conformation and the $C^1(O^1/S^1)C^{\beta}(O^2/S^2)$ and $C^2(O^2/S^2)C^{\beta}(O^1/S^1)$ angles strongly deviate from 60° . The deviation from the *g,g* conformation is also reflected in the significantly narrower $(O^1/S^1)C^{\beta}(O^2/S^2)$ angle than that in the corresponding structures with a constrained *g,g* symmetry where $\angle C^1(O^1/S^1)C^{\beta}(O^2/S^2)$ and $\angle C^2(O^2/S^2)C^{\beta}(O^1/S^1) = 60^\circ$ and a planar C^{α} center ($\angle H^1C^{\beta}C^{\alpha}H^2 = 180^\circ$). It is only slightly wider than that in the structure constrained to the *a,a* symmetry ($\angle C^1(O^1/S^1)C^{\beta}(O^2/S^2)$ and $\angle C^2(O^2/S^2)C^{\beta}(O^1/S^1) = 180.0^\circ$, and $\angle H^1C^{\beta}C^{\alpha}H^2 = 180^\circ$ (Table 1). This angle is somewhat wider in **7h** and **7i**, whose conformation is closer to a *g,g* conformation. However, the structural behavior is not surprising, since the lowest energy conformation is dictated by an interplay between many effects besides the anomeric one, including hyperconjugation with the anionic center, steric effects, and dipole–dipole interactions. Moreover, constraining the $C^{\beta}-X/Z$ bond length might also influence other structural features.

In comparison, the structures of **7en–7in** ($XZCHCH_3$), the neutral conjugate acids of **7e–7i**, reflect very nicely the anomeric effects between X and Z (Table 2). The $C^3(O^1/S^1)C^{\beta}(O^2/S^2)$ and the $C^4(O^2/S^2)C^{\beta}(O^1/S^1)$ angles deviate only slightly from those in the ideal *g,g* conformation where both corresponding angles are 60° . For example, the $C^3(O^1/S^1)C^{\beta}(O^2/S^2)$ and $C^4(O^2/S^2)C^{\beta}(O^1/S^1)$ angles in dimethoxymethane are 64.8° , in agreement with an angle of 63.3° found by electron diffraction.²⁴ The differences in $r(C^{\beta}-O^1/S^1)$ and $r(C^{\beta}-O^2/S^2)$

of the *g,g* conformers (**7a**), where the anomeric interactions are the largest, relative to the corresponding bond lengths of the *a,a* conformers (e.g., **18**), where those interactions are minimal (given in parentheses in Table 2), reflect nicely the contribution of resonance structure **17b**. In the *g,g* conformer of **7en**, $r(C^{\beta}-O^1)$ and $r(C^{\beta}-O^2)$ are only slightly longer than those of the *a,a* conformer, indicating that the shortening of the $C^{\beta}-O^1$ bond due to electron donation from the $2p(O^1)$ lone pair to the $\sigma^*(C^{\beta}-O^2)$ orbital is compensated by its lengthening caused by electron back-donation from the $2p(O^2)$ lone pair to the $\sigma^*(C^{\beta}-O^1)$ orbital. Due to symmetry, the same arguments are valid also for $r(C^{\beta}-O^2)$. Similarly, $r(C^{\beta}-S^1)$ and $r(C^{\beta}-S^2)$ of **7fn** in the *g,g* conformer are almost identical to the corresponding ones in the *a,a* conformer. When the two substituents differ, $r(C^{\beta}-O^1/S^1)$ and $r(C^{\beta}-O^2/S^2)$ are affected differently by the anomeric effect, depending on the competing $p(X/Z) \rightarrow \sigma^*(C-X/Z)$ electron delocalization pathways which are mainly dictated by the energy differences between these two orbitals and by their overlap. According to NBO calculations,¹⁹ the $\sigma^*(C-X)$ orbital energies (eV) in $RXCH_2CH_3$ ($X = O, S$; $R = CH_3, CF_3CH_2$) are: $\sigma^*(C-OCH_3)$ (8.3) > $\sigma^*(C-OCH_2CF_3)$ (8.0) > $\sigma^*(C-SCH_3)$ (4.3). The energy of $\sigma^*(C-X)$ is generally lowered on increasing the electronegativity of X in a given row and on increasing the atomic number within a group.^{11a} The $p(X)$ orbital energies (eV) are $3p(CH_3S)$ (−6.2) > $2p(CH_3O)$ (−7.8) > $2p(CF_3CH_2O)$ (−8.6). In view of the orbital energies given above,²⁵ in **7gn**, a larger electron delocalization is expected from the $2p(O^1)$ orbital to the σ^* -

(24) Astrap, E. E. *Acta Chem. Scand.* **1973**, 27, 3271.

(25) The $p(X) \rightarrow \sigma^*(C^{\beta}-X)$ NBO energy differences are (eV) 12.1 ($2p(CH_3O) \rightarrow \sigma^*(C^{\beta}-SCH_3)$) < 14.5 ($3p(CH_3S) \rightarrow \sigma^*(C^{\beta}-OCH_3)$), 15.8 ($2p(OCH_3) \rightarrow \sigma^*(C^{\beta}-OCH_2CF_3)$) < 16.9 ($2p(CF_3CH_2O) \rightarrow \sigma^*(C^{\beta}-OCH_3)$), and 12.9 ($2p(OCH_2CF_3) \rightarrow \sigma^*(C^{\beta}-SCH_3)$) < 14.2 ($3p(SCH_3) \rightarrow \sigma^*(C^{\beta}-OCH_2CF_3)$).

TABLE 3. Calculated Thermodynamic Stabilization Energies (ΔE ; at B3LYP/6-31++G(d,p)^a + ZPE) of the Most Stable Conformers of XZCHCH₂[−] Calculated by Isodesmic Eqs 4–7 and of their Conjugate Acids (Eq 8)

anion	substituents	reaction energies ΔE (kcal/mol)					
		eq 4	eq 5	eq 6a	eq 6b	eq 7	eq 8
7b	X = CH ₃ O, Z = H	13.0 (−60.8), ^{b,c} 12.0, ^d 10.8 ^{c−e}					
7c	X = CH ₃ S, Z = H	19.4 (−55.5), ^{b,c} 12.0, ^d 10.1 ^{c−e}					
7d	X = CF ₃ CH ₂ O, Z = H	24.2 (−52.3), ^{b,c} 14.2, ^d 11.6 ^{c−e}					
7e	X = Z = CH ₃ O		24.2, 17.2 ^f	11.2		−1.8	7.3 (6.8) ^g
7f	X = Z = CH ₃ S		28.0, 17.5 ^f	8.7		−10.7	1.2 (4.6) ^g
7g	X = CH ₃ O, Z = CH ₃ S		26.4, 18.2 ^f	13.4	7.0	−6.0	3.3 (5.1) ^g
7h	X = CH ₃ O, Z = CF ₃ CH ₂ O		34.7, 19.4 ^f	21.7	10.5	−2.5	7.9 (7.8) ^g
7i	X = CH ₃ S, Z = CF ₃ CH ₂ O		36.7, 20.2 ^f	17.3	12.5	−6.9	3.2 (6.1) ^g

^a Using the B3LYP/6-31++G(d,p) optimized geometries with the constraints described in the text. ^b Free energy of solvation including nonelectrostatic terms. ^c Calculated using the PCM method for modeling a 1:1 DMSO/H₂O solution. ^d HCA calculated from the rotation barrier (**9a** → **10**), not including ZPE. ^e The rotation barriers in **7b**–**7d** calculated using optimized geometries in solution are 10.8, 9.8, and 11.8 kcal/mol, respectively. ^f Hyperconjugative stabilization energies calculated by eq 3, $\theta = 90 + \angle(\text{O}^1/\text{S}^1)\text{C}^\beta\text{C}^\alpha\chi$ or $\angle(\text{O}^2/\text{S}^2)\text{C}^\beta\text{C}^\alpha\chi$. The latter angles are given in Table 1. ^g Anomeric effect in XZCHCH₂CH₃ calculated by $E(g,g) - E(a,a)$, not including ZPE.

(C^β–S²) orbital, while the back-donation will be smaller. This is reflected in the significant lengthening of the C^β–S² bond and the slight shortening of the C^β–O¹ bond relative to the corresponding bonds in the *a,a* conformer. In **7hn** a larger electron delocalization is expected from 2p(O²) in CH₃O to σ*(C^β–O¹CH₂CF₃). Consequently, the C^β–O¹CH₂CF₃ bond is elongated considerably, while the C^β–O²CH₃ bond is hardly changed. In **7in** the C^β–S² bond is elongated by 0.04 Å, while the C^β–O¹CH₂CF₃ bond is only slightly shortened by 0.006 Å, consistent with the smaller energy difference between 2p(O¹) and σ*(C–SCH₃), relative to that between the 3p(S) and σ*(C–OCH₂CF₃) orbitals. The general trend from the data in Table 2 is that the acceptor bond is elongated significantly, while the bond to the donor is only slightly affected.

A third geometric parameter that reflects the anomeric interaction in **7en**–**7in** is the (O¹/S¹)C^β(O²/S²) angle, which is considerably wider in the *g,g* conformation and ranges from 112° to 115° than in the *a,a* conformation, which is ca. 102° (Table 2).

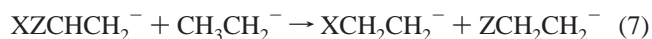
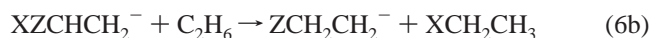
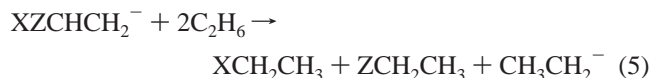
b. Thermodynamic Stability: Monosubstituted Anions. The HCAs in **7b**, **7c**, and **7d** (X = CH₃O, CH₃S, and CF₃CH₂O, respectively) as calculated from the energy required for a rotation around the C^β–C^α bond by 90° (**9a** → **10**) ($\angle\text{H}^1\text{C}^\beta\text{C}^\alpha\text{H}^2 = 180^\circ$) are 12.0, 12.0, and 14.2 kcal/mol, respectively (Table 3), reflecting a very similar HCA for these three anions (a rotation barrier of 0.03 kcal/mol for CH₃CH₂[−] (**7a**) is negligible).²⁶ According to isodesmic reaction 4, the thermodynamic



stabilization of these anions relative to **7a** (X = H) and to their conjugate acids is 13.0, 19.4, and 24.2 kcal/mol, respectively (Table 3). The large difference for **7c** and **7d** between the hyperconjugative stabilization energies calculated from the rotation barriers and the stabilization energy calculated by reaction 4 indicates that the 2p(C^α) → σ*(C^β–X) hyperconjugative interaction is not the only factor that affects the anion stability and that other factors (e.g., field effects) have a significant effect (ca. 10 kcal/mol for **7d**, X = CF₃CH₂O). We note that the energies of isodesmic reaction 4 for **7b**–**7d** actually reflect the difference in the calculated gas-phase acidities of CH₃OCH₂CH₃, CH₃SCH₂CH₃, and CF₃CH₂OCH₂CH₃ of 403.5,

398.8, and 393.9 kcal/mol, respectively, with the latter being the most acidic and its conjugate base CF₃CH₂OCH₂CH₂[−] being the most stable. According to PCM calculations in 1:1 DMSO/H₂O, the HCAs (calculated from the rotation barriers) are 10.8, 10.1, and 11.6 kcal/mol for **7b**–**7d**, respectively, showing only a small solvent effect. The calculations also show that the free energies of solvation of **7d** (X = CF₃CH₂O) and **7c** (X = CH₃S) are 8.5 and 5.3 kcal/mol smaller than that of **7b** (X = CH₃O) (Table 3), decreasing the stabilities of **7d** and **7c** relative to **7b** in solution in comparison with their gas-phase stabilities, leading to a slightly higher stability of **7d** than those of the other two ions. These differences in solvation energies are exhibited in the differences between the gas-phase and solution acidities of CH₃OCH₂CH₃, CH₃SCH₂CH₃, and CF₃CH₂OCH₂CH₃. The calculated acidity of CF₃CH₂OCH₂CH₃ in solution is larger than that of CH₃OCH₂CH₃ by 4 kcal/mol ($\Delta\text{p}K_a = 2.9$), while in the gas phase it is larger by 10 kcal/mol. This decrease in the acidity difference in solution is in agreement with the smaller solvation energy of its conjugate base (**7d**) relative to that of **7b**. A similar trend was found experimentally for the relative acidities of CF₃CH₂OH and CH₃OH. In the gas phase the former is 15 kcal/mol more acidic than the latter, but the difference in water is only 4 kcal/mol.^{21a–c,27}

What is the effect of a second CH₃O, CH₃S, or CF₃CH₂O C^β substituent on the total stability of carbanions **7e**–**7i**? To answer this question, we have calculated the energies of bond separation reactions 5–8 using the optimized most stable



XZCHCH₂[−] conformers (Table 3). Again, the energies of bond separation reactions reflect the sum of all stabilizing and destabilizing effects and not of a specific interaction and reflect

(26) A significantly smaller stabilizing effect is caused by the interaction between the lone pairs on O and S and the σ*(C–CH₂[−]) orbital. Its contribution to the stability of **7b** and **7c** is calculated to be ca. 2.0 kcal/mol.

(27) (a) $\text{p}K_a(\text{in H}_2\text{O}) = 15.5$ and 12.4 for CH₃OH and CF₃CH₂OH, respectively.^{21b,c} (b) Bartmess, J. E.; Scott, J. A.; McIver, R. T., Jr. *J. Am. Chem. Soc.* **1979**, *101*, 6056. (c) F. G. Bordwell, *Acc. Chem. Res.* **1988**, *21*, 456.

also the relative stabilities of the compounds in the right-hand side of the equations.^{11g}

Reaction 5 exhibits the thermodynamic stabilization in the disubstituted anions **7e–7i** relative to CH_3CH_2^- and to the corresponding monosubstituted neutral ethers and/or sulfides. In these disproportionation reactions the X and Z substituents are being separated from each other and from the anionic center, thus canceling both the negative hyperconjugation and anomeric stabilizations. The energies of these reactions also include a release of steric repulsion between the geminal substituents in the anions, which we assume to be ca. 2–3 kcal/mol for the methylthio-substituted anions (see below). According to these reactions, the total stabilization is 24.2, 28.0, and 26.4 kcal/mol for **7e–7g**, respectively, and it is considerably larger, 35–36 kcal/mol, for the $\text{CF}_3\text{CH}_2\text{O}$ -substituted anions **7h** and **7i**. In **7e–7g** most of the stabilization results from the contribution of the hyperconjugative interaction of X and Z with the CH_2^- group. These hyperconjugative stabilization energies (calculated using eq 3, Table 3) are very similar for **7e–7i** and are in the range of 17–20 kcal/mol. The contribution of the mutual anomeric interaction between the X and Z substituents is very small. A conformational analysis shows a very flat PES for rotation around the $\text{X/Z}-\text{C}^\beta$ bonds and that only ca. 1 kcal/mol separates the various conformations. For example, for **7e**, a local minimum conformer with $\text{C}^1(\text{O}^1)\text{C}^\beta(\text{O}^2)$ and $\text{C}^2(\text{O}^2)\text{C}^\beta(\text{O}^1)$ dihedral angles of 55.8° and 86.9° (close to the *g,g* conformation) and a local minimum conformer with $\text{C}^1(\text{O}^1)-\text{C}^\beta(\text{O}^2)$ and $\text{C}^2(\text{O}^2)\text{C}^\beta(\text{O}^1)$ dihedral angles of -174.0° and 171.0° (close to the *a,a* conformation), respectively, are only ca. 1 kcal/mol higher in energy than the lowest energy conformer presented in Table 1. From the above, we conclude that the larger total stabilization calculated (eq 5) for **7h** and **7i** reflects mainly stabilizing field effects of the $\text{CF}_3\text{CH}_2\text{O}$ group rather than hyperconjugative or anomeric effects (see the discussion of the energies of eq 4 for anions **7b–7d**).

Reactions 6a and 6b reflect the extra stabilization gained when a hydrogen on C^β in $\text{XC}^\beta\text{H}_2\text{C}^\alpha\text{H}_2^-$ is replaced by a Z substituent bearing lone pair electrons:²⁸ More stabilization is gained when H in $\text{CH}_3\text{OCH}_2\text{CH}_2^-$ is replaced by either CH_3O or CH_3S (11.2 and 13.4 kcal/mol for **7e** and **7g**, respectively; eq 6a, Table 3) than when the C^β hydrogen in $\text{CH}_3\text{SCH}_2\text{CH}_2^-$ is replaced by the same substituents, leading to a stabilization of 8.7 and 7.0 kcal/mol (eqs 6a (**7f**) and 6b (**7g**), respectively). The higher endothermicities of reaction 6a ($\text{X} = \text{Z} = \text{CH}_3\text{O}$) than of reaction 6a ($\text{X} = \text{Z} = \text{CH}_3\text{S}$) or reaction 6b ($\text{X} = \text{CH}_3\text{O}$ and $\text{Z} = \text{CH}_3\text{S}$) reflects in part the higher stability of the monosubstituted anions **7c** vs **7b** as calculated by reaction 4. A considerably larger stabilization of 21.7 kcal/mol (eq 6a with $\text{X} = \text{CH}_3\text{O}$ and $\text{Z} = \text{CF}_3\text{CH}_2\text{O}$) and 17.3 kcal/mol (eq 6a with $\text{X} = \text{CH}_3\text{S}$ and $\text{Z} = \text{CF}_3\text{CH}_2\text{O}$) is gained when $\text{CF}_3\text{CH}_2\text{O}$ replaces the hydrogen in $\text{CH}_3\text{OCH}_2\text{CH}_2^-$ or $\text{CH}_3\text{SCH}_2\text{CH}_2^-$, respectively. These large values reflect the slightly larger HCA of $\text{CF}_3\text{CH}_2\text{O}$ relative to CH_3O and CH_3S shown by the rotation barrier, but they mainly reflect other stabilizing effects (as shown also for **7d**). The lower endothermicities of reaction 6b relative to reaction 6a (with $\text{X} = \text{CH}_3\text{O}$ and CH_3S and $\text{Z} = \text{CF}_3\text{CH}_2\text{O}$)

manifest the higher stability of $\text{CF}_3\text{CH}_2\text{OCH}_2\text{CH}_2^-$ relative to $\text{CH}_3\text{OCH}_2\text{CH}_2^-$ and $\text{CH}_3\text{SCH}_2\text{CH}_2^-$ (eq 4) or the higher acidity of $\text{CF}_3\text{CH}_2\text{OCH}_2\text{CH}_3$ relative to $\text{CH}_3\text{OCH}_2\text{CH}_3$ and $\text{CH}_3\text{SCH}_2\text{CH}_3$. In summary, reactions 5 and 6 demonstrate that the C^β -disubstituted anions are considerably more stable than the respective monosubstituted anions, as also shown by the hyperconjugative stabilization energies calculated from eq 3. However, as shown by eq 7 a disubstituted anion is less stable than the sum of two monosubstituted anions as is also predicted from eq 3.

In reaction 8 we present the anomeric stabilization in the neutral conjugate acids **7en–7in**. It is the largest (kcal/mol) between two RO substituents (7.3 and 7.9 for **7en** and **7in**, respectively), it is smaller between an RO and a CH_3S substituent (3.3 and 3.2 for **7gn** and **7in**, respectively), and it is only 1.2 between two CH_3S substituents. The anomeric effect was also calculated from the energy difference between the *g,g* and *a,a* conformers (Table 3, in parentheses). The anomeric stabilization energies calculated by the isodesmic reaction and from rotation around the $\text{C}^\beta-\text{X}$ and $\text{C}^\beta-\text{Z}$ bonds are almost the same when X and Z are both RO groups (ca. 7 and 8 kcal/mol in **7e** and **7h**, respectively), but a discrepancy of 2–3 kcal/mol is found when one or both groups are CH_3S . This can be partially attributed to a larger steric repulsion between geminal substituents involving the larger sulfur atom. This steric repulsion is relieved on the right-hand side of the isodesmic equation, leading to an apparent lower anomeric stabilization relative to that calculated from the rotation energies. Accordingly, the largest deviation is found for $(\text{CH}_3\text{S})_2\text{CHCH}_3$. We thus estimate that the upper limit of destabilization of **7fn**, **7gn**, and **7in** (and in their corresponding anions) due to steric repulsion is ca. 3 kcal/mol.^{7a,d}

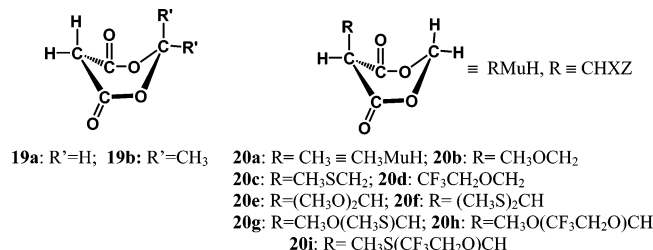
In conclusion, the stability of **7b–7d** ($\text{X} = \text{CH}_3\text{O}$, CH_3S , $\text{CF}_3\text{CH}_2\text{O}$, $\text{Z} = \text{H}$) relative to **7a** ($\text{X} = \text{Z} = \text{H}$) (eq 4) decreases in the following order: **7d** ($\text{X} = \text{CF}_3\text{CH}_2\text{O}$) > **7c** ($\text{X} = \text{CH}_3\text{S}$) > **7b** ($\text{X} = \text{CH}_3\text{O}$) (Table 3, entries **7b–7d**). This stabilization is mainly attributed to the hyperconjugation of the lone pair of electrons in the $2p(\text{C}^\alpha)$ orbital with the $\sigma^*(\text{C}-\text{X})$ orbital (**7**). However, the significantly larger stabilization energy of **7d** ($\text{X} = \text{CF}_3\text{CH}_2\text{O}$) calculated by isodesmic reaction 4 than that calculated from the rotation barrier indicates that for **7d** other stabilization effects, besides HCA are important. In solution, this additional stabilization is less important and the stabilities of the three ions **7b–7d** are very similar. Substituting C^β in **7b–7d** by CH_3O or CH_3S increases their stability by 9–13 kcal/mol. This increase is mainly attributed to the increase in the additional negative hyperconjugation between the $2p(\text{C}^\alpha)$ orbital and the $\sigma^*(\text{C}^\beta-\text{Z})$ orbital. The anomeric interaction between X and Z is estimated to be relatively small.

B. Meldrum's Acid-like Substituted Anions XZCHMu^- (8a–8i**).** Meldrum's acid (**19b**) has an exceptionally high acidity²⁹ ($\text{pK}_a = 7.3^{29b}$ in DMSO and 4.8 in water^{29c}). It is 11.7

(28) (a) In all reactions where the substituents are being separated from each other, we have to consider the release of steric repulsion between the geminal X and Z substituents. (b) The lower stability of **8f** ($\text{X} = \text{Z} = \text{CH}_3\text{S}$) may result in part from a larger steric repulsion between the two alkylthio substituents relative to that between two alkoxy substituents or an alkoxy and an alkylthio substituent.^{7a,d}

(29) (a) Meldrum, A. N. *J. Chem. Soc., Trans.* **1908**, 93, 598. (b) Arnett, E. M.; Maroldo, S. L.; Harrelson, J. A., Jr. *J. Am. Chem. Soc.* **1984**, 106, 6759. (c) Eigen, M.; Ilgenfritz, G.; Kruse, W. *Chem. Ber.* **1965**, 98, 1623. (d) Bunting, J. W.; Kanter, J. P.; Nelander, R.; Wu, Z. *Can. J. Chem.* **1995**, 73, 1305. (e) Wiberg, K. B.; Laidig, K. E. *J. Am. Chem. Soc.* **1988**, 110, 1872. (f) Wang, X.; Houk, K. N. *J. Am. Chem. Soc.* **1988**, 110, 1870. (g) Byun, K.; Mo, Y.; Gao, J. *J. Am. Chem. Soc.* **2001**, 123, 3974. (h) Lee, I.; Han, I.-S.; Kim, C.-K.; Lee, H.-W. *Bull. Korean Chem. Soc.* **2003**, 24, 1141. (i) Nakamura, S.; Hirao, H.; Ohwada, T. *J. Org. Chem.* **2004**, 69, 4309. (j) Mishima, M.; Matsuoka, M.; Lei, Y.-X.; Rappoport, Z. *J. Org. Chem.* **2004**, 69, 5947.

kcal/mol^{29g} more acidic than dimethyl malonate ($pK_a = 15.9^{29b}$ in DMSO and 13.0 in water^{29d}). It was used to stabilize the anions generated in the first step of representative S_NV reactions (eq 1), thus letting them accumulate to concentrations that allow measurements of k_1 , k_{-1} , and K_1 . In our calculations we use models of Meldrum's acid derivatives, lacking the *gem*-dimethyl group, that is, **20a–20i** and their conjugate bases, anions **8a–8i**. Since **19a** and **19b** have very similar structural and electronic



properties (although calculations show that **19a** is ca. 2 kcal/mol more acidic than **19b**),^{29hj} we believe that these models are reliable for analyzing the effects of **19b** on the stability of the corresponding intermediates in S_NV reactions.

a. Geometry. The fully optimized geometries of the most stable conformations of **8a–8i** and those of their conjugate acids **20a–20i** are given in Tables 4 and 5, respectively.

In contrast to anions **7a–7i**, the anionic center in **8a–8i** is almost planar, i.e., $\angle C^1C^\alpha C^\beta C^{22}$ is ca. 168° , reflecting an anionic charge delocalization into the Meldrum's acid (Mu) moiety (see below). In the monosubstituted anions **8b–8d** the $X-C^\beta$ bond almost eclipses the $2p(C^\alpha)$ orbital as shown by the $(O/S)C^\beta C^\alpha C^{22}$ dihedral angles, enabling good overlap and interaction between the $2p(C^\alpha)$ and $\sigma^*(C^\beta-X)$ orbitals. The $C^\beta-C^\alpha$ bond lengths in **8a–8i** are 1.49–1.50 Å, significantly shorter than the corresponding bond lengths in the conjugate acids **20a–20i** of ca. 1.54 Å. The $C^\beta-C^\alpha$ bond lengths in monosubstituted anions **8b–8d** are 1.2%, 2.1%, 2.8%, and 2.2% shorter than the corresponding bonds in **20a–20d**. Those in the disubstituted anions **8e–8i** are shorter by ca. 3% than the corresponding bonds in **20e–20i** (Tables 4 and 5), reflecting a higher degree of negative hyperconjugation in the disubstituted ions (see below). On the other hand, the $O/S-C^\beta$ bonds in **8a–8i** are longer than those in the corresponding neutrals. These geometric features reflect nicely a contribution of resonance structure **9b**, which exhibits hyperconjugation between the $2p(C^\alpha)$ and $\sigma^*(C^\beta-O/S)$ orbitals. Figure 1 shows that in **8b–8d** the $C^\beta-C^\alpha$ bonds become shorter and the $X-C^\beta$ bonds are elongated upon rotation of X about the $C^\beta-C^\alpha$ bond from $\angle(O^1/S^1)C^\beta C^\alpha C^{22} = 180.0^\circ$, where these orbitals are out of phase and hyperconjugation is not possible, to $\angle(O^1/S^1)C^\beta C^\alpha C^{22}$ of ca. 90.0° , where the $2p(C^\alpha)$ orbital almost eclipses the $\sigma^*(C^\beta-X)$ orbital.

The structural rule outlined above that predicts rotamer **13** ($\theta_X = 60^\circ$) to be of the highest stability according to eq 3 is only approximately valid for the disubstituted anions **8e–8i** as exhibited by $\angle(O^1/S^1)C^\beta C^\alpha C^{33}$ and $\angle(O^2/S^2)C^\beta C^\alpha C^{33}$ (Table 4).

Is the mutual anomeric effect between X and Z reflected in the geometry? The most stable optimized structures have an approximate *g,g* conformation as shown by the dihedral angles $C^1(O^1/S^1)C^\beta(O^2/S^2)$ and $C^2(O^2/S^2)C^\beta(O^1/S^1)$ (Table 4). However, due to the significant elongation of the O^1/S^1-C^β and O^2/S^2-C^β bonds caused by the negative hyperconjugation, a systematic analysis of the effect of the anomeric interaction between X and Z on these bond lengths is not possible. Nevertheless, the

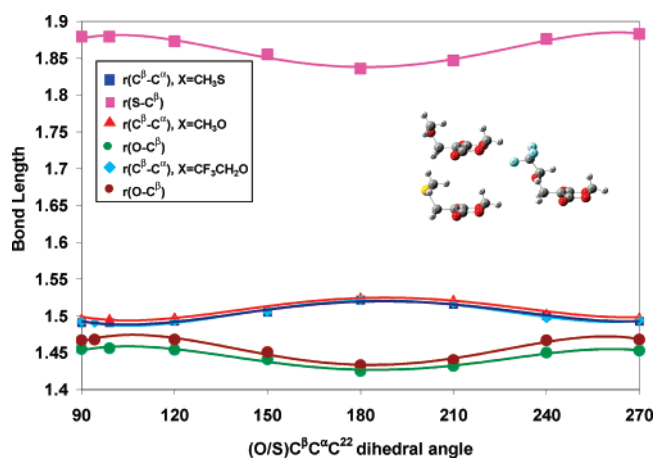


FIGURE 1. Change in $r(C^\beta-C^\alpha)$ and $r(O/S-C^\beta)$ bond lengths in XCH_2Mu^- (**8b–8d**) as a function of the $(O/S)C^\beta C^\alpha C^{22}$ dihedral angle (calculated at B3LYP/6-31++G(d,p)). The dihedral angle was kept constant at each point, while all other geometry parameters were fully optimized. Atom numbering is according to structure **A** in Table 4.

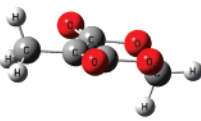
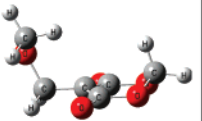
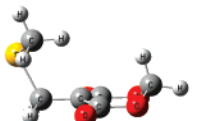
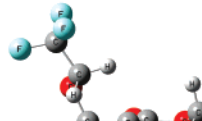
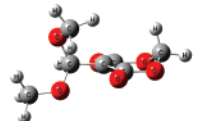
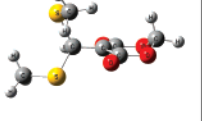
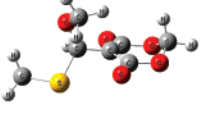
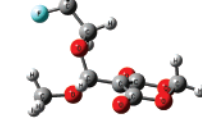
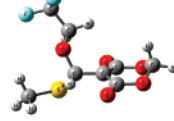
significant broadening of the $(O^1/S^1)C^\beta(O^2/S^2)$ angle, from ca. 100° in the *a,a* conformer (i.e., with $\angle C^1(O^1/S^1)C^\beta(O^2/S^2) = 180.0^\circ$ and $\angle C^2(O^2/S^2)C^\beta(O^1/S^1) = 180.0^\circ$) to ca. 110° in the fully optimized approximate *g,g* conformer, resembles the broadening of these angles in neutral **20e–20i** (Table 5) pointing to the existence of the mutual anomeric interaction.

In **20e–20i** (which have an approximate *g,g* conformation) the $C^\beta-C^\alpha$ bond lengths are significantly shorter than those in the restricted *a,a* conformations (Table 5). The bond elongation in the *a,a* conformation reflects a strong hyperconjugation (or anomeric effect) between the $2p(O/S)$ lone pairs and the $\sigma^*(C^\beta-C^\alpha)$ orbital which is stabilized by the electronegative Mu substituent. This interaction is possible in the *a,a* conformers due to the more favorable orientation of their $2p(O/S)$ lone pairs relative to the $C^\beta-C^\alpha$ bond, as exhibited by the $C^3(O^1/S^1)C^\beta C^\alpha$ and $C^4(O^2/S^2)C^\beta C^\alpha$ dihedral angles (Table 5). NBO analysis indeed shows a significant second-order perturbation (SOP) stabilization between the $2p(O/S)$ lone pairs of both X and Z groups and the $\sigma^*(C^\beta-C^\alpha)$ orbital. For example, in the *a,a* conformer of **20e** the SOP stabilization resulting from the interaction of both CH_3O groups with the $\sigma^*(C^\beta-C^\alpha)$ orbital is 21 kcal/mol. In contrast, in the optimal structure the stabilization energy is only ca. 8 kcal/mol, resulting from the interaction of only one CH_3O substituent, while the interaction with the second CH_3O group is silent.

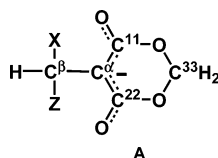
The optimized $C^3(O^1/S^1)C^\beta(O^2/S^2)$ and $C^4(O^2/S^2)C^\beta(O^1/S^1)$ dihedral angles in **20e–20i** deviate from the ideal *g,g* conformation (ca. 64.0° calculated for **7en–7in**, Table 2), decreasing the stabilization from the mutual anomeric effect, but this effect is probably compensated by other stabilizing conjugative and steric effects. The overall structure reflects a balance of various electronic and steric effects.

To estimate the contribution of a mutual anomeric effect between X and Z , we compare $r(C^\beta-O^1/S^1)$ and $r(C^\beta-O^2/S^2)$ in the optimal structures (**20e–20i**) with those in the corresponding restricted *a,a* structures (where such interaction is not possible). We have to remember that these bonds are also shortened due to hyperconjugation between the X and Z lone pairs and the $\sigma^*(C^\beta-C^\alpha)$ orbital, an effect that is more significant in the *a,a* conformers (see above). In **20e** the $C^\beta-O$ bond lengths are similar in both conformations,

TABLE 4. Schematic Structures and Selected Geometry Parameters^a for $XZCHMu^-$ (X, Z = H, CH_3O , CH_3S , and CF_3CH_2O)^{b,c}

Geometry parameters	 8a	 8b	 8c	 8d	
$r(C^\beta-C^\alpha)$	1.508	1.497	1.491	1.491	
$r(O/S-C^\beta)$	1.102 ^{d,e}	1.456	1.879	1.468	
$r(C^1-O/S)$	—	1.411	1.827	1.398	
$\angle(O/S)C^\beta C^\alpha$	112.69 ^d	116.03	116.99	115.90	
$\angle C^1(O/S)C^\beta C^\alpha$	—	-66.0	-62.1	-62.1	
$\angle(O/S)C^\beta C^\alpha C^{33\ f}$	-179.9 ^d	-0.2	1.1	-3.0	
$\angle(O/S)C^\beta C^\alpha C^{22}$	84.0	98.6	99.2	94.2	
$\angle C^{11}C^\alpha C^\beta C^{22}$	168.2	167.1	166.8	166.3	
Geometry parameters	 8e	 8f	 8g	 8h	 8i
$r(C^\beta-C^\alpha)$	1.503 (1.507)	1.496 (1.491)	1.499 (1.496)	1.499 (1.503)	1.495 (1.492)
$r(O^1/S^1-C^\beta)$	1.439 (1.430)	1.879 (1.874)	1.436 (1.433)	1.455 (1.446)	1.452 (1.446)
$r(O^2/S^2-C^\beta)$	1.427 (1.426)	1.860 (1.879)	1.876 (1.881)	1.417 (1.417)	1.864 (1.875)
$r(C^1-O^1/S^1)$	1.422 (1.409)	1.826 (1.824)	1.420 (1.412)	1.408 (1.395)	1.405 (1.399)
$r(C^2-O^2/S^2)$	1.412 (1.412)	1.829 (1.826)	1.832 (1.826)	1.418 (1.413)	1.832 (1.826)
$\angle(O^1/S^1)C^\beta(O^2/S^2)$	110.0 (101.2)	112.12 (103.3)	110.2 (100.9)	109.5 (100.9)	109.9 (100.8)
$\angle(O^1/S^1)C^\beta C^\alpha C^{33\ f}$	-34.8 (-44.0)	-23.0 (-47.0)	-24.7 (-53.3)	37.8 (40.4)	27.1 (53.5)
$\angle(O^2/S^2)C^\beta C^\alpha C^{33\ f}$	-161.6 (-161.9)	-155.4 (-170.1)	-154.5 (-172.5)	164.7 (158.2)	156.4 (172.8)
$\angle C^1(O^1/S^1)C^\beta(O^2/S^2)$	72.8 (180.0)	67.7 (180.0)	76.4 (180.0)	-69.7 (180.0)	-74.2 (180.0)
$\angle C^2(O^2/S^2)C^\beta(O^1/S^1)$	62.4 (180.0)	72.2 (180.0)	70.3 (180.0)	-65.6 (180.0)	-69.7 (180.0)
$\angle C^1(O^1/S^1)C^\beta C^\alpha$	-54.5 (54.2)	-65.5 (50.0)	-55.2 (52.7)	57.6 (-53.4)	57.2 (-51.9)
$\angle C^2(O^2/S^2)C^\beta C^\alpha$	-167.2 (-54.6)	-153.5 (-50.3)	-156.8 (-52.6)	164.7 (55.0)	158.2 (53.0)
$\angle C^{11}C^\alpha C^\beta C^{22}$	168.4 (171.0)	169.1 (170.9)	168.8 (171.5)	167.6 (170.4)	168.0 (170.9)

^a Bond lengths in angstrom, bond angles in degrees, at B3LYP/6-31++G(d,p). ^b For the most stable conformer. The values in parentheses are for the less stable *a,a* conformer where $\angle C^1(O^1/S^1)C^\beta(O^2/S^2)$ and $\angle C^2(O^2/S^2)C^\beta(O^1/S^1)$ were frozen at 180.0°. ^c For the atom numbering use the following formulas and structure A: **8a**, $H^0C^\beta H_2C^\alpha C^{11}C^{22-}$; **8b**, $C^1H_3OC^\beta H_2C^\alpha C^{11}C^{22-}$; **8c**, $C^1H_3SC^\beta H_2C^\alpha C^{11}C^{22-}$; **8d**, $CF_3C^1H_2OC^\beta H_2C^\alpha C^{11}C^{22-}$; **8e**, $C^1H_3O^1(C^2H_3O^2)C^\beta H_2C^\alpha C^{11}C^{22-}$; **8f**, $C^1H_3O^1(C^2H_3S^2)C^\beta H_2C^\alpha C^{11}C^{22-}$; **8g**, $C^1H_3S^1(C^2H_3O^2)C^\beta H_2C^\alpha C^{11}C^{22-}$; **8h**, $CF_3C^1H_2O^1(C^2H_3O^2)C^\beta H_2C^\alpha C^{11}C^{22-}$; **8i**, $CF_3C^1H_2O^1(C^2H_3S^2)C^\beta H_2C^\alpha C^{11}C^{22-}$. O^1/S^1 and O^2/S^2 are located above and below the $C^\beta C^\alpha C^{11}C^{22}$ plane, respectively.

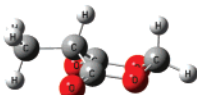
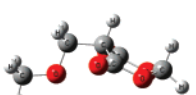
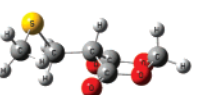
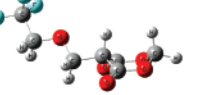
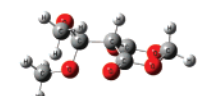
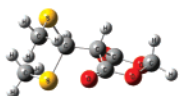
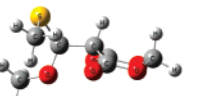
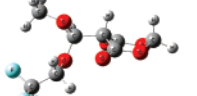
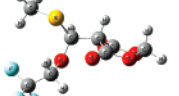


^d $r(H^0-C^\beta)$, $\angle H^0C^\beta C^\alpha$, $\angle H^0C^\beta C^\alpha C^{11}$, and $\angle H^0C^\beta C^\alpha C^{33}$, respectively. ^e $r(H-C^\beta) = 1.095 \text{ \AA}$. ^f Used as a measure of the deviation from eclipsing $2p(C^\alpha)$ and $\sigma^*(C^\beta-O/S)$ orbitals.

indicating that the shortening of the $C^\beta-O^1$ bond due to electron donation from the $2p(O^1)$ lone pair to the $\sigma^*(C^\beta-O^2)$ orbital is compensated by its lengthening caused by electron back-donation from the $2p(O^2)$ lone pair to the $\sigma^*(C^\beta-O^1)$ orbital. Due to symmetry the same arguments are valid also for $r(C^\beta-O^2)$. Similarly, the differences between $r(C^\beta-S^1)$ and $r(C^\beta-S^2)$ of **20f** and those of its *a,a* conformer are

also very small. In **20g**, in view of the relative $2p(O/S) \rightarrow \sigma^*(C^\beta-O/S)$ orbital energies (see above and ref 25), a larger electron delocalization is expected from the $2p(O^2)$ orbital to the $\sigma^*(C^\beta-S^1)$ orbital, while the back-donation from the $2p(S^1)$ orbital to the $\sigma^*(C^\beta-O^2)$ orbital will be smaller. This is reflected in a significant lengthening of 0.013 Å of the $C^\beta-S^1$ bond and the slight shortening by 0.005 Å of the $C^\beta-O^2$

TABLE 5. Schematic Structures and Selected Calculated Geometry Parameters^a of XZCHMuH (X, Z = H, CH₃O, CH₃S, CF₃CH₂O) (**20**)^b

Geometry parameters	 20a , R = C ^β H ₂ H ⁰	 20b , R = C ¹ H ₃ O ¹ C ^β H ₂	 20c , R = C ¹ H ₃ S ¹ C ^β H ₂	 20d , R = CF ₃ C ¹ H ₂ O ¹ C ^β H ₂	
$r(\text{C}^{\beta}\text{-C}^{\alpha})$	1.527	1.530	1.535	1.525	
$r(\text{C}^{\beta}\text{-O}^1/\text{S}^1)$	1.092 ^c	1.412	1.837	1.424	
$\angle \text{C}^1(\text{O}^1/\text{S}^1)\text{C}^{\beta}\text{C}^{\alpha}$	-	-179.9	169.4	-99.0	
Geometry parameters	 20e , R = C ³ H ₃ O ¹ (C ⁴ H ₃ O ²)C ^β H	 20f , R = C ³ H ₃ S ¹ (C ⁴ H ₃ S ²)C ^β H	 20g , R = C ³ H ₃ S ¹ (C ⁴ H ₃ O ²)C ^β H	 20h , R = C ³ H ₃ O ¹ (CF ₃ C ⁴ H ₂ O ²)C ^β H	 20i , R = C ³ H ₃ S ¹ (CF ₃ C ⁴ H ₂ O ²)C ^β H
$r(\text{C}^{\beta}\text{-C}^{\alpha})$	1.553 (1.608)	1.544 (1.552)	1.541 (1.560)	1.549 (1.578)	1.548 (1.556)
$r(\text{C}^{\beta}\text{-O}^1/\text{S}^1)$	1.409 (1.390)	1.850 (1.850)	1.863 (1.850)	1.395 (1.395)	1.839 (1.849)
$r(\text{C}^{\beta}\text{-O}^2/\text{S}^2)$	1.397 (1.393)	1.841 (1.848)	1.397 (1.402)	1.422 (1.403)	1.422 (1.409)
$r(\text{C}^3\text{-O}^1/\text{S}^1)$	1.434 (1.418)	1.828 (1.827)	1.831 (1.827)	1.435 (1.417)	1.831 (1.827)
$r(\text{C}^4\text{-O}^2/\text{S}^2)$	1.428 (1.424)	1.828 (1.828)	1.428 (1.424)	1.419 (1.408)	1.417 (1.413)
$\angle (\text{O}^1/\text{S}^1)\text{C}^{\beta}(\text{O}^2/\text{S}^2)$	114.7 (103.1)	116.5 (103.3)	115.1 (102.5)	114.8 (102.7)	117.1 (102.0)
$\angle \text{C}^3(\text{O}^1/\text{S}^1)\text{C}^{\beta}(\text{O}^2/\text{S}^2)$	50.4 (180.0)	48.8 (180.0)	42.4 (180.0)	-78.3 (180.0)	-78.3 (180.0)
$\angle \text{C}^4(\text{O}^2/\text{S}^2)\text{C}^{\beta}(\text{O}^2/\text{S}^2)$	71.6 (180.0)	86.7 (180.0)	76.5 (180.0)	-32.4 (180.0)	-36.5 (180.0)
$\angle \text{C}^3(\text{O}^1/\text{S}^1)\text{C}^{\beta}\text{C}^{\alpha}$	-74.9 (57.7)	-84.3 (53.0)	-84.8 (56.1)	154.2 (57.8)	151.2 (56.0)
$\angle \text{C}^4(\text{O}^2/\text{S}^2)\text{C}^{\beta}\text{C}^{\alpha}$	-159.5 (-58.8)	-138.9 (-54.5)	-152.4 (-57.3)	92.0 (-58.2)	93.5 (-57.3)

^a Bond lengths in angstroms, bond angles in degrees, at B3LYP/6-31++G(d,p). ^b For the most stable conformer. Values in parentheses are for the less stable *a,a* conformer in which ∠C³(O¹/S¹)C^β(O²/S²) and ∠C⁴(O²/S²)C^β(O²/S²) are frozen to 180.0°. ^c r(C^β-H⁰).

bond relative to the corresponding bonds in the *a,a* conformer. In **20h** a larger electron delocalization is expected from the 2p(CH₃O¹) orbital to the σ*(C^β-O²CH₂CF₃) orbital, with a consequent considerable C^β-O²CH₂CF₃ bond elongation while the C^β-O¹CH₃ bond length remains unchanged. In **20i** the C^β-S¹ bond is slightly shortened by 0.01 Å while the C^β-O²CH₂CF₃ bond is elongated by 0.013 Å, in contrast with the expectation from the energy differences between 2p(CF₃CH₂O) and σ*(C-SCH₃) (12.9 eV) orbitals, and between 3p(CH₃S) → σ*(C-OCH₂CF₃) (14.2 eV) orbitals. Another parameter that points to the existence of an anomeric interaction in **20e**–**20i** is the (O¹/S¹)C^β(O²/S²) angle, which is considerably wider (115–117°) in the optimal conformation, relative to that in the *a,a* conformation, of ca. 102–103° (Table 5).

b. Thermodynamic Stability. 1. Stabilization of the Anions by the Mu Group at C^α. The anions **8a**–**8i** are the conjugate bases of substituted analogues of Meldrum's acids (**20**). The high acidity of the latter has a strong implication on the relative thermodynamic stabilities of these anions. The gas-phase acidities of compounds **20** calculated using eq 9 (Table



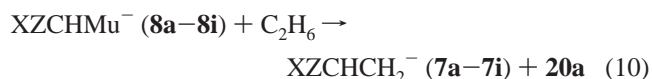
6) show that the acidity increases upon monosubstitution and follows the order CF₃CH₂O > CH₃S > CH₃O and that an additional CH₃O substituent does not affect the acidity. This order reflects the stability order of the conjugate bases (see below).

TABLE 6. Calculated Stabilization Energies (Δ*E*) Caused by Meldrum's Acid-like Substituent in Anions **8a**–**8i**^{a,b} and the Gas-Phase Acidity of Their Conjugate Acids **20**^{a,c}

anion	X	Z	Δ <i>E</i>	acidity of 20
8a	H	H	92.9	325.2
8b	H	CH ₃ O	82.2	319.8
8c	H	CH ₃ S	79.0	317.3
8d	H	CF ₃ CH ₂ O	78.4	311.5
8e	CH ₃ O	CH ₃ O	75.9	319.8
8f	CH ₃ S	CH ₃ S	69.2	315.9
8g	CH ₃ S	CH ₃ O	71.0	317.4
8h	CH ₃ O	CF ₃ CH ₂ O	71.4	311.2
8i	CH ₃ S	CF ₃ CH ₂ O	67.8	308.0

^a In kilocalories per mole. ^b According to eq 10. ^c Δ*H* at 0 K for reaction 9. A higher endothermicity reflects a lower acidity of **20** and a higher basicity of their conjugate bases **8**.

The stabilization energy (Δ*E*) of anions **8a**–**8i** caused by the Mu substituent at C^α is calculated using isodesmic eq 10 and is summarized in Table 6.



The extremely high stabilization of 68–93 kcal/mol explains the accumulation of the anions in the experimental studies.^{7b–d} It is attributed to efficient conjugation between 2p(C^α) and the vicinal carbonyl groups of the Mu moiety, as shown in Table 7 for **8b**–**8d**. For example, in **7b** the occupancy¹⁹ in the 2p(C^α) orbital is 1.78 electrons, while in **8b** it is only 1.34 electrons, and 0.38 electrons are delocalized into each of the π*(C=O)

TABLE 7. Conjugative Stabilization Energies (ΔE_{ij} , kcal/mol),^a Energy Differences between the $2p(C^\alpha)$ and $\sigma^*(C^\beta-X)$ Orbitals and between the $2p(C^\alpha)$ and $\pi^*(C=O)$ Orbitals ($\epsilon_j - \epsilon_i$), and NBO Occupancies (electrons) in $2p(C^\alpha)$, $\sigma^*(C^\beta-X)$, and $\pi^*(C=O)$ in $XCH_2YY'^-$ ($X = CH_3O$, CH_3S , and CF_3CH_2O , **7b–7d** and **8b–8d**, Respectively)

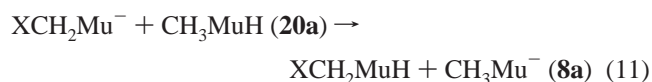
X	ΔE_{ij} ($i = 2p(C^\alpha)$, $j = \sigma^*(C^\beta-X)$)	ΔE_{ij} ($i = 2p(C^\alpha)$, $j = \pi^*(C=O)$)	$\epsilon_j - \epsilon_i$ ($i = 2p(C^\alpha)$, $j = \sigma^*(C^\beta-X)$)	$\epsilon_j - \epsilon_i$ ($i = 2p(C^\alpha)$, $j = \pi^*(C=O)$)	$F(ij)^b$ (au) ($i = 2p(C^\alpha)$, $j = \sigma^*(C^\beta-X)$)	occupancy in $2p(C^\alpha)$ NBO	occupancy in $\sigma^*(C^\beta-X)$ NBO	occupancy in $\pi^*(C=O)$ NBO
Y, Y' = H								
H (7a)	11.5		14.4		0.071	1.86	0.074	
CH ₃ O (7b)	26.0		11.7		0.096	1.78	0.13	
CH ₃ S (7c)	27.3		7.9		0.081	1.72	0.195	
CF ₃ CH ₂ O (7d)	28.6		11.2		0.1	1.75	0.150	
YY' = Mu								
H (8a)	7.5	105.2, 105.2	14.7	4.1	0.070	1.32	0.017	0.4, 0.4
CH ₃ O (8b)	18.3	103.0, 99.7	10.3	4.1	0.089	1.34	0.053	0.38, 0.37
CH ₃ S (8c)	18.2	102.3, 98.4	6.5	4.1	0.070	1.33	0.061	0.39, 0.37
CF ₃ CH ₂ O (8d)	19.6	98.5, 94.2	9.8	4.4	0.090	1.35	0.059	0.38, 0.36

^a Stabilization energy estimated by second-order perturbation theory. $\Delta E_{ij} = q_i(F(ij))^2/(\epsilon_j - \epsilon_i)$; see ref 19b for details. ^b Fock matrix element, indicative of the overlap between the orbitals.

orbitals of the Mu moiety. In **7b** the total charge on C^α is -1.0 electrons (and on the $C^\alpha H_2$ group it is -0.71 electron), while in **8b** C^α carries a total *positive charge* of $+0.41$ electron, and the total charge on Mu^- is -0.6 electron (the negative charge resides on its four oxygen atoms). The charge delocalization is manifested in a very large donor–acceptor stabilization energy (calculated by second-order perturbation theory^{19b}) of ca. 100 kcal/mol. The stabilization caused by Mu^- (eq 10) is the largest for the unsubstituted anion **8a** and is higher for the monosubstituted anions **8b–8d** than for the disubstituted anions **8e–8i**. The stabilization is lower for anions substituted by CF_3CH_2O . This trend is also followed by the second-order perturbation stabilization energy shown in Table 7. CF_3CH_2O increases the $\epsilon_{\pi^*(C=O)} - \epsilon_{2p(C^\alpha)}$ energy difference and thereby lowers the donor–acceptor stabilization.

2. Stabilization Due to Hyperconjugation in **8b–8d.** A secondary and significantly smaller stabilizing effect is due to the hyperconjugation between the $2p(C^\alpha)$ and $\sigma^*(C^\beta-X)$ orbitals. The hyperconjugative stabilization energies calculated by the rotation barrier, i.e., $\angle XC^\beta C^\alpha C^{22} \approx 90.0^\circ \rightarrow \angle XC^\beta C^\alpha C^{22} \approx 180^\circ$ (see atom numbering in Table 4), are 8.5, 7.6, and 7.5 kcal/mol for $X = CH_3S$, CH_3O , and CF_3CH_2O , smaller than those calculated for the parent anions **7c**, **7b**, and **7d**, of 12.0, 12.0, and 14.2 kcal/mol, respectively. This trend is also in agreement with the corresponding smaller relative second-order perturbation energies, ΔE_{ij} ($i = 2p(C^\alpha)$, $j = \sigma^*(C^\beta-X)$), Table 7), in **8b–8d** and is also exhibited by the lower electron occupancy in the $\sigma^*(C-X)$ orbitals of **8b–8d** vs those of **7b–7d**. All these reflect the decrease of the charge on C^α caused by charge delocalization over the Mu fragment (Table 7). The calculated rotation barriers (HCAs) in 1:1 DMSO/H₂O solution are similar, i.e., 6.5, 7.0, and 6.7 kcal/mol, for **8b–8d**, respectively.

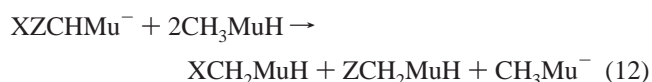
The total thermodynamic stability of XCH_2Mu^- (**8b–8d**), relative to the unsubstituted anion **8a** and to the corresponding substituted **20**, calculated by isodesmic eq 11 (Table 8) decrease



in the order (kcal/mol) **8d** ($X = CF_3CH_2O$, 12.9) > **8c** ($X = CH_3S$, 7.0) > **8b** ($X = CH_3O$, 5.4), obeying the same trend as, but with considerably smaller values than, the relative thermodynamic stabilities of **7d**, **7c**, and **7b** of 24.2, 19.4, and 13.0 kcal/mol, respectively (reaction 4). Note the higher thermody-

namic stabilities of **8d** and **7d**, which are consistent with the higher acidity of **20d** ($R = CF_3CH_2OCH_2$), relative to those of **20b** and **20c** ($R = CH_3OCH_2$ and $R = CH_3SCH_2$). This contrasts with the very similar HCAs caused by all three substituents calculated from rotation barriers (Tables 3 and 8) and the similar second-order perturbation energies (ΔE_{ij}) for **7b–7d** as well as for **8b–8d** (Table 7). These observations indicate that for **7d** and **8d** hyperconjugation does not play an exclusive role in their stabilization. The relatively large differences in the total stability among **8d**, **8c**, and **8b** become smaller (but the trend is kept) in 1:1 DMSO/H₂O solution since the free energy of solvation of **8b** is 5.3 and 3.0 kcal/mol more stabilizing than those of **8d** and **8c**, respectively (Table 8).

3. Disubstituted Anions **8e–8i.** The thermodynamic stabilities of the disubstituted anions **8e–8i** are analyzed by isodesmic eqs 12–14. The calculated reaction energies in the gas phase and in solution and the free energies of solvation in 1:1 DMSO/H₂O solution are given in Table 8.



When one of the C^β hydrogens in **8b–8d** is replaced by CH_3O or CH_3S , the resulting disubstituted anions are thermodynamically more stable (relative to their neutral conjugate acids) than the monosubstituted anions (Table 8). Reaction 12 evaluates the total stabilities of $XZCHCHMu^-$ (**8e–8i**) relative to the sum of the corresponding monosubstituted conjugate acids **20b–20d** and the parent anion **8a**. The energies of these reactions reflect the hyperconjugation between the C^α lone pair and the $\sigma^*(C-X)$ and $\sigma^*(C-Z)$ orbitals, the anomeric interactions between X and Z, and other stabilizing effects (e.g., field effects). They also reflect a destabilization of the disubstituted anions caused by steric repulsion between the geminal X and Z substituents.^{28a} The following trend in stability is found in the gas phase: **8h** > **8i** > **8e** > **8g** > **8f**. The most stable anions are those substituted by CF_3CH_2O , and the least stable is the anion substituted by two CH_3S groups.^{28b} The low stability of

TABLE 8. Stabilization Energies (ΔE , at B3LYP/6-31++G(d,p) + ZPE)^{a,b} Calculated Using Isodesmic Reactions 11–14 in the Gas Phase and in Solution;^c Stabilization Due to Hyperconjugation (H)^{b,c,d} and the Anomeric Effect (A)^{b,c,e} and Free Energy of Solvation (ΔG_{solv})^{b,c} of the Most Stable Conformers of Anions XZCHMu^- (**8b–8i**)

anion	substituents	ΔE					H	A^f	ΔG_{solv}
		reaction 11	reaction 12	reaction 13a	reaction 13b	reaction 14			
8b	X = CH ₃ O, Z = H	5.4 (1.7)					7.5 ^g (6.5) ^g		−55.0
8c	X = CH ₃ S, Z = H	7.5 (3.2)					8.5 ^g (7.0) ^g		−52.0
8d	X = CF ₃ CH ₂ O, Z = H	12.9 (5.8)					7.6 ^g (6.7) ^g		−49.7
8e	X = Z = CH ₃ O		11.6 (4.1) ^h	6.2 (2.4) ^h	6.2 (2.4) ^h	0.8 (0.7) ^h	11.8	2.4 (1.7)	−55.1
8f	X = Z = CH ₃ S		8.4 (0.6) ^h	0.9 (−2.6) ^h	0.9 (−2.6) ^h	−6.6 (−5.8) ^h	14.2	2.8 (2.5)	−49.9
8g	X = CH ₃ O, Z = CH ₃ S		9.5 (1.3) ^h	4.1 (−0.5) ^h	2.0 (4.1) ^h	−3.4 (−3.6) ^h	13.1	3.2 (2.4)	−51.8
8h	X = CH ₃ O, Z = CF ₃ CH ₂ O		19.6 (5.4) ^h	14.2 (3.7) ^h	6.7 (4.1) ^h	1.3 (0.5) ^h	11.8	3.9 (2.3)	−48.9
8i	X = CH ₃ S, Z = CF ₃ CH ₂ O		16.7 (2.2) ^h	9.2 (−0.9) ^h	3.8 (4.1) ^h	−3.7 (−4.2) ^h	13.1	4.4 (3.2)	−46.2

^a Using the B3LYP/6-31++G(d,p)-optimized geometries. ^b In kilocalories per mole. ^c Values in parentheses and ΔG_{solv} are calculated for a 1:1 DMSO/H₂O solution at the gas-phase geometries, using the PCM model with UAHF radii and including nonelectrostatic energies. ^d Calculated using eq 3, neglecting the hyperconjugation with $\sigma^*(\text{C}^\beta\text{--H})$. $\theta_X = \angle(\text{O}^1/\text{S}^1)\text{C}^\beta\text{C}^\alpha\text{C}^{33} + 90.0$, $\theta_Z = \angle(\text{O}^2/\text{S}^2)\text{C}^\beta\text{C}^\alpha\text{C}^{33} + 90.0$ (for values see Table 4). ^e Anomeric stabilization calculated from the energy difference between the energy of the *a,a* conformer (e.g., **18**) and that of the optimal structure. ^f Anomeric stabilization energies in the conjugate acids **20e–20i** are 8.4, 8.9, 9.3, and 8.0 kcal/mol, respectively. ^g HCA calculated from the rotation barrier (**9a** → **10**), not including ZPE. ^h Reflecting the solvation energies of all reactants and products.

8f is attributed to a larger destabilization caused by the steric repulsion between the bulkier geminal methylthio substituents (Table 8; see detailed analysis below). The stabilization energies of anions **8e–8i** are significantly smaller than those calculated for the parent anions **7e–7i**, similarly to the situation discussed above for the monosubstituted anions **8b–8d** vs **7b–7d**. In solution we find that the solvation free energy is more stabilizing for **8e** (X = Z = CH₃O, −55.1 kcal/mol), **8g** (X = CH₃O, Z = CH₃S, −51.8 kcal/mol), and **8f** (X = CH₃S, Z = CH₃S, −49.9 kcal/mol) than for **8i** (X = CH₃S, Z = CF₃CH₂O, −46.2 kcal/mol) and **8h** (X = CH₃O, Z = CF₃CH₂O, −48.9 kcal/mol), reducing significantly the difference in stability calculated in the gas phase between **8h** and **8i** and all other ions and making **8e** more stable than **8i**. This indicates that in a 1:1 DMSO/H₂O solution the stabilizing polar effects in **8i** and **8h** become less important in dictating the stability order. The estimated trend of the stabilities in solution is **8h** > **8e** > **8i** > **8g** > **8f**; the most stable ions are those substituted by two alkoxy groups, and the stability is smaller for ions substituted by one and two methylthio groups.

Can we estimate the individual contribution of hyperconjugative and anomeric effects and of polar (field effects) and steric effects to the total stabilization calculated by reaction 12? To do so, we calculated the hyperconjugative stabilization energies by using eq 3 and the anomeric effects by rotating the X and Z substituents from their optimal geometry to an *a,a* conformation (i.e., **17a** → **18**); the resulting energies H and A , respectively, are given in Table 8. The results of this analysis show that the contribution of negative hyperconjugation is significantly larger than that of the anomeric effects. The difference between the energies of reaction 12 and the sum of conjugative energies (negative hyperconjugation and anomeric effect, denoted as $H + A$) gives an estimation of the contribution of the steric effects and of polar effects. For **8e** the total stabilization (eq 12) is smaller than $H + A$ by 2.6 kcal/mol, indicating some destabilization, probably due to a small steric repulsion between the methoxy groups. For **8f** the total stabilization energy is smaller than $H + A$ by 8.6 kcal/mol, indicating a significantly larger steric effect between the two methylthio groups. Using the same argument, a steric effect of 6.0 kcal/mol destabilizes **8g**. The total stabilization of **8h** is larger by 3.9 kcal/mol than the contribution of $H + A$; taking into account a small steric destabilization (similar to that in **8e**), we can assume a field effect contribution to the stability of **8h** of ca. 6 kcal/mol. A

similar field effect is estimated for **8i**. To sum up, the largest contribution to the stability comes from negative hyperconjugation. Significant destabilizing steric effects are estimated for ions substituted by methylthio groups. Field effects stabilize the ions substituted by CF₃CH₂O, but these become less important in solution. The contribution of the anomeric effect is the smallest, and it is significantly smaller than in the corresponding conjugate acids (Table 8). Note that the contribution of $H + A$ is similar in the gas phase and in solution.

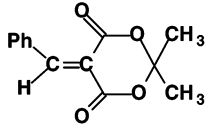
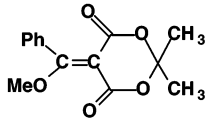
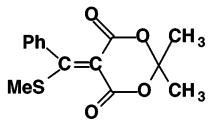
Reactions 13a and 13b reflect the additional stability of the disubstituted anion relative to the monosubstituted anion caused by an additional hyperconjugative $2p(\text{C}^\alpha) \rightarrow \sigma^*(\text{C}^\beta\text{--X})$ and $\sigma^*(\text{C}^\beta\text{--Z})$ interaction and the anomeric effect between X and Z. They also reflect a destabilization caused by the steric repulsion between the geminal C^β substituents.^{28a}

This additional stabilization reflects the difference in stability of the intermediate anions in S_NV reactions of **3-H** vs those of **3-LG** (LG = CH₃O, CH₃S, and CF₃CH₂O). The largest additional stabilization is when both substituents are alkoxy groups, it decreases for anions where one of the substituents is CH₃S, and it is negligible when both substituents are CH₃S. Taking into account (a) the similar HCAs of CH₃S, CH₃O, and CF₃CH₂O (Table 8, H for **8b–8d**) and (b) the trend in the anomeric effects in the ions (kcal/mol), **8i** (4.4) > **8h** (3.9) > **8g** (3.2) > **8f** (2.8) > **8e** (2.4) (Table 8; in solution, **8i** (3.9) > **8f** (2.5) ≈ **8g** (2.4) ≈ **8h** (2.3) > **8e** (1.7)), we conclude similarly to the conclusion based on eq 12 that the larger steric effects in **8g**, **8i**, and **8f**, which are substituted by one or two CH₃S groups, dictate their smaller additional stabilizations. The higher additional stabilization of **8h** relative to **8e** and of **8i** relative to **8g** may be attributed to the contribution of field effects caused by CF₃CH₂O in **8h** and **8i**. The importance of this effect is reduced significantly in solution (Table 8). Equation 14 shows that the disubstituted anions are less stable than the sum of the stabilities of the two monosubstituted anions for X and Z = CH₃S and CH₃S, CH₃S and CH₃O, and CH₃S and CF₃CH₂O,²⁸ but they are slightly more stable for X and Z = CH₃O and CH₃O and CF₃CH₂O and CH₃O.

4. Stability of the Alkene Precursor of the S_NV Reaction.

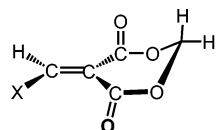
The kinetics of the S_NV reactions is also determined by the stability of the alkene precursors. We thus estimate (a) the stabilizing effects of the Mu substituent on ethylene and its alkoxy and methylthio derivatives **21a–d** using isodesmic eq 15. This reaction shows that the substituted alkenes **21a–d** are

TABLE 9. Experimental Equilibrium Constants (K_1^{Nu}) for the Addition of $\text{HOCH}_2\text{CH}_2\text{S}^-$, $\text{CF}_3\text{CH}_2\text{O}^-$, and OH^- , Respectively, to Benzyldene Meldrum's Acid Derivatives in 1:1 DMSO/ H_2O at 20 °C

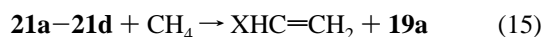
Reactant	$K_1^{\text{HOCH}_2\text{CH}_2\text{S}^-} (\text{M}^{-1})$	$K_1^{\text{CF}_3\text{CH}_2\text{O}^-} (\text{M}^{-1})$	$K_1^{\text{OH}^-} (\text{M}^{-1})$
 (3-H)^a	5.38×10^{10}	6.43×10^6	1.15×10^{10}
 (3-OMe)^b	2.57×10^4	6.81×10^4	1.28×10^8
 (3-SMe)^c	3.32×10^2	2.86×10^1	$\approx 5.1 \times 10^4$

^a Reference 7b. ^b Reference 7c. ^c Reference 7d.

8.9 (X = H), 12.2 (X = CH_3O), 14.8 (X = CH_3S), and 9.8 (X = $\text{CF}_3\text{CH}_2\text{O}$) kcal/mol, respectively, more stable than the corresponding $\text{HXC}=\text{CH}_2$ alkenes (significantly smaller than the stabilization of the intermediate ions caused by the Mu moiety (Table 6)).

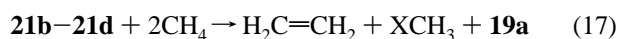


21a: X = H, **21b:** X = CH_3O
21c: X = CH_3S , **21d:** X = $\text{CF}_3\text{CH}_2\text{O}$



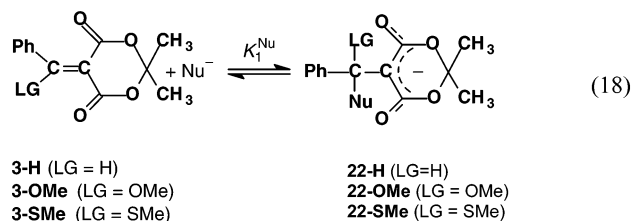
The stabilization of **21a** caused by substituting the vinylic hydrogen by CH_3O , $\text{CF}_3\text{CH}_2\text{O}$, and CH_3S is calculated by eq 16, according to which **21b**, **21c**, and **21d** are more stable than **21a** by 15.2 (X = CH_3O), 12.9 (X = CH_3S), and 11.8 (X = $\text{CF}_3\text{CH}_2\text{O}$) kcal/mol, respectively, reflecting the weaker π -donor stabilizing effect of CH_3S relative to that of CH_3O .^{30,31}

According to eq 17, stabilization of ethylene by both the Mu and X substituents is more significant, being 24.1 (X = CH_3O), 21.8 (X = CH_3S), and 20.6 (X = $\text{CF}_3\text{CH}_2\text{O}$) kcal/mol.



C. Comparison of the Experimental and Computational Results. How do our computational results compare with experimental observations? Table 9 reports equilibrium constants for the reactions of **3-LG** with $\text{HOCH}_2\text{CH}_2\text{S}^-$, $\text{CF}_3\text{CH}_2\text{O}^-$,

and OH^- , respectively (eq 18). Prior to our computational study, the trends in these values were attributed to the interplay of



steric crowding in the intermediate, π -donor and inductive effects of the nucleofuge, and anomeric effects as follows. The two former effects reduce the equilibrium constant, the first by intermediate destabilization and the second by substrate stabilization. In contrast, the inductive and anomeric effects enhance the equilibrium constant by stabilizing the intermediate, the latter being mainly important in the reactions of **3-OMe** with oxanions.

Specifically, for the reactions of **3-OMe** and **3-SMe** with the thiolate ion, the steric effect appears to be dominant as seen by the strongly reduced equilibrium constants relative to that for **3-H** ($K_1^{\text{RS}}(\mathbf{3-OMe})/K_1^{\text{RS}}(\mathbf{3-H}) = 4.78 \times 10^{-7}$ and $K_1^{\text{RS}}(\mathbf{3-SMe})/K_1^{\text{RS}}(\mathbf{3-H}) = 6.17 \times 10^{-9}$).

The fact that $K_1^{\text{RS}}(\mathbf{3-SMe})$ is 77.4-fold smaller than $K_1^{\text{RS}}(\mathbf{3-OMe})$ shows that the bulkier MeS group adds to the overall steric effect; this additional steric effect is too large to be offset by the considerably weaker π -donor effect of the MeS group compared with the MeO group^{30,31} although the stronger inductive effect of the MeO group contributes somewhat to the larger $K_1^{\text{RS}}(\mathbf{3-OMe})$ value.

For the reactions of $\text{CF}_3\text{CH}_2\text{O}^-$ or OH^- the equilibrium constants for **3-OMe** and **3-SMe** are not as strongly depressed relative to those for **3-H** ($K_1^{\text{CF}_3\text{CH}_2\text{O}}(\mathbf{3-OMe})/K_1^{\text{CF}_3\text{CH}_2\text{O}}(\mathbf{3-H}) = 1.06 \times 10^{-2}$, $K_1^{\text{CF}_3\text{CH}_2\text{O}}(\mathbf{3-SMe})/K_1^{\text{CF}_3\text{CH}_2\text{O}}(\mathbf{3-H}) = 6.17 \times 10^{-6}$, $K_1^{\text{OH}}(\mathbf{3-OMe})/K_1^{\text{OH}}(\mathbf{3-H}) = 1.11 \times 10^{-2}$, $K_1^{\text{OH}}(\mathbf{3-SMe})/K_1^{\text{OH}}(\mathbf{3-H}) = 4.43 \times 10^{-6}$). Here the smaller size of the oxanion nucleophile reduces the steric crowding in the respective

intermediates. These trends are in agreement with the additional stability calculated by reactions 13a and 13b in solution (Table 8). The difference between the equilibrium constants of reactions of **3-OMe** and **3-SMe** with alkoxy ions is much larger than in the thiolate ion reaction, i.e., $K_1^{\text{CF}_3\text{CH}_2\text{O}}(\textbf{3-OMe})/K_1^{\text{CF}_3\text{CH}_2\text{O}}(\textbf{3-SMe}) = 2.38 \times 10^3$ and $K_1^{\text{OH}}(\textbf{3-OMe})/K_1^{\text{OH}}(\textbf{3-SMe}) = 2.51 \times 10^3$ as compared to $K_1^{\text{RS}}(\textbf{3-OMe})/K_1^{\text{RS}}(\textbf{3-SMe}) = 77.4$. This was attributed to a much stronger anomeric effect between the leaving group and the nucleophile in dialkoxy intermediates than in alkoxy(alkylthio) or bis(alkylthio) intermediates. The results of our calculations now require a revision of these earlier interpretations. Specifically and most importantly, the computational results imply that the anomeric effect plays only a minor role in stabilizing the intermediates. Moreover, it is not greater for the dialkoxy intermediates than for the alkoxy(methylthio) and bis(alkylthio) intermediates, and thus, it does not significantly increase the stability of the respective intermediates. Furthermore, the HCAs are also similar for the alkoxy- and alkylthio-substituted anions. Hence, we conclude that the differences in the equilibrium constants mentioned above, which are in agreement with the differences in the total stabilization energies calculated by eq 12 for **8e–8i** in the gas phase and in solution (Table 8), are mainly due to steric destabilization of the intermediates which are substituted by one or two alkylthio substituents (the slightly larger hyperconjugative stabilization of the anions substituted by methylthio groups does not compensate their steric destabilization). The calculations show that the additional stabilization of **8e–8i** does not compensate for the π -donor stabilization in the precursor alkenes, but the larger additional stabilization of **8e** and **8h** (Table 8, reactions 13a and 13b) accounts for the significantly smaller ratio of $K_1^{\text{CF}_3\text{CH}_2\text{O}}(\textbf{3-H})/K_1^{\text{CF}_3\text{CH}_2\text{O}}(\textbf{3-MeO})$ (94) relative to $K_1^{\text{HOCH}_2\text{CH}_2\text{S}}(\textbf{3-H})/K_1^{\text{HOCH}_2\text{CH}_2\text{S}}(\textbf{3-MeO})$ (2.1×10^6). The calculations show that a MeO group stabilizes the substrate (**3-OMe**) more than a methylthio group (**3-SMe**), in line with earlier conclusions based on experimental data.

Conclusions. The electron-withdrawing Mu at C $^\alpha$ stabilizes the S_NV intermediates considerably and allows their accumulation and the kinetic measurement of their formation and decomposition.

(30) For example, $\sigma_{\text{R}}(\text{CH}_3\text{O})$ of -0.43^{31} is much more negative than $\sigma_{\text{R}}(\text{CH}_3\text{S})$ of -0.15^{31} .

(31) Hansch, C.; Leo, A.; Taft, R. W. *Chem. Rev.* **1991**, *91*, 165.

The second important stabilizing factor of these ions is the negative hyperconjugation stabilization, which is similar for ions **8e–8i**, and follows the trend (in kcal/mol) for **8e–8i**. It follows the trend (in kcal/mol) **8f** (X = Z = CH₃S, 14.2) > **8g** (X = CH₃O, Z = CH₃S, 13.1) = **8i** (X = CF₃CH₂O, Z = CH₃S, 13.1) > **8e** (X = Z = CH₃O, 11.8) = **8i** (X = CF₃CH₂O, Z = CH₃O, 11.8), in agreement with the higher HCA of CH₃S (Table 8). The HCAs in **8b–8d** are significantly smaller than in **7b–7d** due to charge delocalization in the Mu moiety in the former. Consequently, the total thermodynamic stabilization (relative to neutral counterparts and **7a** or **8a**) of anions **8b–8i** is significantly smaller than that of **7b–7i**.

In the gas phase the most stabilized ions (**7** or **8**) are those in which one of the substituents is CF₃CH₂O. Their higher stabilization is attributed to polar effects (e.g., field effects). These effects become less important in solution where the solvation energy of the CF₃CH₂O-substituted ions is smaller than that of the CH₃O-substituted ions, resulting in a similar stability for ions **8h** and **8e** or **8i** and **8g** (Table 8).

The mutual anomeric effect contributes significantly less to the stability of these ions being in the range of 2–4 kcal/mol. These anomeric effects are significantly smaller than those in the neutral conjugate acids **20e–20i** of ca. 8–9 kcal/mol because in the anions the acceptor $\sigma^*(\text{C-X/Z})$ orbitals are already partially occupied due to negative hyperconjugation with the anionic center, probably showing a saturation phenomenon. Solvent effects on the hyperconjugative and anomeric stabilizing energies are small.

Steric effects play an important role in destabilizing the ions which are substituted by methylthio groups and consequently affect the trends in the equilibrium constants of the S_NV reaction.

Acknowledgment. This study was supported by the U.S.-Israel Binational Science Foundation (BSF) and the Minerva Foundation in Munich (M.K., Z.R.). C.F.B. thanks the National Science Foundation for its support through Grant No. CHE-0446622.

Supporting Information Available: Complete ref 22 and optimized Cartesian coordinates and total energies of **7a–7i** and **8a–8i** and their corresponding conjugate acids **7an–7in** and **20a–20i**. This material is available free of charge via the Internet at <http://pubs.acs.org>.

JO7017476